Published in final edited form as:
Hear Res. 2007 February ; 224(1-2): 34–50.

Genetic Dependence of Cochlear Cells and Structures Injured by Noise

Kevin K. Ohlemiller* and **Patricia M. Gagnon**
Department of Otolaryngology, Washington University School of Medicine, Saint Louis, MO 63110

Abstract

The acute and permanent effects of a single damaging noise exposure were compared in CBA/J, C57BL/6 (B6), and closely related strains of mice. Two hrs of broadband noise (4–45 kHz) at 110 dB SPL led to temporary reduction in the endocochlear potential (EP) of CBA/J and CBA/CaJ (CBA) mice and acute cellular changes in cochlear stria vascularis and spiral ligament. For the same exposure, B6 mice showed no EP reduction and little of the pathology seen in CBA. Eight weeks after exposure, all mice showed a normal EP, but only CBA mice showed injury and cell loss in cochlear lateral wall, despite the fact that B6 sustained larger permanent threshold shifts. Examination of noise injury in B6 congenics carrying alternate alleles of genes encoding otocadherin (Cdh23), agouti protein, and tyrosinase (albinism) indicated that none of these loci can account for the strain differences observed. Examination of B6xCBA F1 mice and F1xB6 N2 mice further indicated that susceptibility to noise-related EP reduction and associated cell pathology are inherited in an autosomal dominant manner, and are established by one or a few large effect quantitative trait loci. Findings support a common genetic basis for an entire constellation of noise related cochlear pathologies in cochlear lateral wall and spiral limbus. Even within species, cellular targets of acute and permanent cochlear noise injury may vary with genetic makeup.

Keywords

Stria vascularis; spiral ligament; spiral limbus; endocochlear potential; fibrocytes; C57BL/6; CBA/J; melanin

Introduction

The cellular correlates of cochlear noise injury in mammals have been intensively studied reviews:(Salvi et al., 1982; Slepecky, 1986; Saunders et al., 1991; Borg et al., 1995). From many reports, consensus has emerged concerning both the reversible changes that may underlie transient aspects of hearing loss and irreversible changes associated with permanent hearing loss. Reversible changes may include altered spatial relations within the organ of Corti (Beagley, 1965; Harding et al., 1992; Nordmann et al., 2000), injury to hair cell stereocilia (Liberman and Kiang, 1978; Liberman and Mulroy, 1982; Liberman and Dodds, 1984), injury to afferent dendrites (Robertson, 1983; Puel et al., 1998), and transient depression of the endocochlear potential (EP) (Syka et al., 1981). Irreversible changes causing permanent

*Correspondence to: Kevin K. Ohlemiller, Ph.D., Department of Otolaryngology, Washington University, 660, S. Euclid, St. Louis, MO 63110, (314) 747-7179, fax: 314-747-7230, e-mail: kohlemiller@wustl.edu.

Funding Agencies: NIH R01 DC03454 (KKO), NIH P30 DC04665

hearing loss appear concentrated in the organ of Corti, and dominated by hair cell loss and non-lethal hair cell injury e.g.,(Covell, 1953; Johnson and Hawkins, 1976; Hamernik et al., 1989; Ou et al., 2000a; Wang et al., 2002). Wang et el. (Wang et al., 2002) and Hirose and colleagues (Hirose and Liberman, 2003; Hirose et al., 2005) characterized noise injury in CBA/CaJ mouse cochlea extending beyond the organ of Corti to stria vascularis, spiral ligament, and spiral limbus. Acute changes in the cochlear lateral wall were associated with temporary reduction of the EP. Although the EP usually recovered, injury to the lateral wall and spiral limbus was permanent. While such injury may not contribute directly to permanent hearing loss, it may promote ongoing degeneration and accelerate apparent aging processes in the cochlea.

Comparative studies generally suggest that species differences among mammals in cochlear noise injury are largely quantitative (Saunders and Tilney, 1980) rather than qualitative, and support the proposition that there exists an essentially 'mammalian' character of cochlear noise injury. The availability of genetically distinct strains of rats and mice have made these useful for discovering genetic contributions to the *severity* of noise injury. Within rats (Borg, 1982; Axelsson et al., 1983) and mice (Henry, 1982; Li, 1992; Erway et al., 1996; Yoshida et al., 2000; Candreia et al., 2004; Vazquez et al., 2004), different strains show marked variation in noise susceptibility. In mice, moreover, several genetic loci that can mediate such differences are known e.g., (Ohlemiller et al., 1999; Ohlemiller et al., 2000; Davis et al., 2001; Kozel et al., 2002; Davis et al., 2003). Little evidence, however, has been presented for *qualitative* differences in noise injury within or across mammalian species. In a follow-up study to the studies of Liberman, Wang, Hirose, and their colleagues (Wang et al., 2002; Hirose and Liberman, 2003), we obtained very different results in C57BL/6J (B6) mice (Ohlemiller et al., 2003). For noise exposure similar to that applied to CBA/CaJ mice, B6 mice show no significant acute EP reduction. This result seemed paradoxical, since B6 mice are known to be more vulnerable to noise-induced threshold shifts than are CBAs (Erway et al., 1993; Erway et al., 1996; Johnson et al., 1997; Davis et al., 2001). We speculated that the cellular targets of noise differ in these two strains, such that organ of Corti is more noise susceptible in B6, while the cochlear lateral wall is more susceptible in CBAs.. If that is true, then genes that modulate noise injury to the organ of Corti versus other structures may exert their influence independently, and any single metric used to compare two strains or individuals may provide an incomplete picture. Here we examine how cochlear stria vascularis, spiral ligament, and spiral limbus of CBA and B6 mice differ in their response to damaging noise. We also explore the underlying genetics using informative congenic models, as well as B6/CBA F1 hybrid and N2 backcross mice to B6.

Materials and Methods

Animals

All procedures were approved by the Washington University Institutional Animal Care and Use Committee. The basic procedure involved exposing inbred, congenic, and hybrid mice one time to broadband noise followed by hearing assessment and recording of the endocochlear potential (EP), and sacrifice for histology 1–3 hrs, 24 hrs, or 8 wks after exposure. All groups were roughly evenly balanced by gender. Mice were purchased directly from The Jackson Laboratory (JAX) or were derived from breeders purchased from JAX. Ages and group sizes by test condition are given in Table I. Subjects included CBA/J (CBA), CBA/CaJ, and C57BL/6J (B6) inbred mice, plus congenics to B6 as follows: B6.CAST-*Cdh23*^{CAST} (B6.CAST), C57BL/6-*Tyr*$^{c\text{-}2J}$ (albino), and C57BL/6J-*A*$^{w\text{-}J}$ (white-bellied agouti). Also included were B6/CBA F1 hybrids and [(B6.CAST/CBA) x B6.CAST] N2 backcross mice.

B6 mice carry the *Cdh23*^{ahl} allele, which promotes progressive hearing loss and exacerbates noise injury (Erway et al., 1993; Erway et al., 1996; Johnson et al., 1997; Davis et al., 2001). Results from congenic B6.CAST-*Cdh23*^{CAST} mice (which do not carry this allele) demonstrate

that the presence of this allele on the B6 background did not influence our main findings. Nevertheless, in generating our N2 backcross mice, it seemed advisable to eliminate any possible influence of the *Cdh23*^{ahl} allele. For this reason, N2 mice were generated using B6.CAST mice exclusively. In the production of F1 and N2 mice, male parents were always CBA.

CAP recording

Compound action potential (CAP) recordings were conducted as terminal procedures, such that each animal was assessed once immediately prior to sacrifice. Animals were anesthetized (60 mg/kg sodium pentobarbital, IP) and positioned ventrally in a custom headholder. Core temperature was maintained at 37.5 ± 1.0°C using a thermostatically-controlled heating pad in conjunction with a rectal probe (Yellow Springs Instruments Model 73A). An incision was made along the midline of the neck and soft tissues were blunt dissected and displaced laterally to expose the trachea and animal's left bulla. A tracheostomy was then made and the musculature over the bulla was cut posteriorly to expose the bone overlying the round window. Using a hand drill, a small hole was made over the round window. The recording electrode was a modified platinum needle electrode (Grass) insulated with epoxy except for the tip, which was inserted into round window antrum using a micromanipulator. Additional platinum electrodes inserted into the neck musculature and hind leg served as reference and ground, respectively. Electrodes were led to a Grass P15 differential amplifier (100–3,000 Hz, x100), then to a custom amplifier providing another x1,000 gain, then digitized at 30 kHz using a Cambridge Electronic Design Micro1401 in conjunction with SIGNAL^{TM} and custom signal averaging software operating on a 120 MHz Pentium PC. Sinewave stimuli generated by a Hewlett Packard 3325A oscillator were shaped by a custom electronic switch to 5 ms total duration, including 1 ms rise/fall times. The stimulus was amplified by a Crown D150A power amplifier and output to a KSN1020A piezo ceramic speaker located 7 cm directly lateral to the left ear. Stimuli were presented freefield and calibrated using a B&K 4135 ¼ inch microphone placed where the external auditory meatus would normally be. Toneburst stimuli at each frequency and level were presented 100 times at 3/sec. The minimum sound pressure level required for visual detection of a response (N_1) was determined at 5, 10, 20, 28.3, and 40 kHz, using a 5 dB minimum step size. Two-way ANOVA was used to compare CAP thresholds after noise in CBA/J and B6.CAST-*Cdh23*^{CAST} mice (Fig. 6A).

Endocochlear potential recording

The EP was measured using a ventral approach immediately after CAP recording. Using a fine drill, a hole was made in the left cochlear capsule directly over scala media of both lower basal and apical turns. Glass capillary pipettes (40–80 MΩ) filled with 0.15 M KCl were mounted on a hydraulic microdrive (Frederick Haer) and advanced until a stable positive potential was observed that did not change with increased electrode depth. The signal from the recording electrode was led to an AM Systems Model 1600 intracellular amplifier. EP differences by condition and strain were compared by t-test, since noise-exposed animals were compared only with non-exposed controls of the same strain (Figs. 2A, 6B, 9B, 10). Linear relations between basal and apical turn EP, and between basal turn EP and CAP thresholds were tested by Pearson correlation (Figs. 2B, 12A,B).

Tissue processing for histology

At the end of recording, animals were overdosed and perfused transcardially with cold 2.0% paraformaldehyde/2.0% glutaraldehyde in 0.1 M phosphate buffer (pH 7.4). Each cochlea was rapidly isolated, immersed in the same fixative, and the stapes was immediately removed. Complete infiltration of the cochlea by fixative was ensured by making a small hole at the apex of the cochlear capsule, and gently circulating the fixative over the cochlea using a transfer

pipet. After decalcification in sodium EDTA for 72 hours, cochleas were post-fixed in buffered 1% osmium tetroxide, dehydrated in an ascending acetone series, and embedded in Epon. Cochleas were sectioned in the mid-modiolar plane at 4.0 μm, then stained with toluidine blue for bright field viewing with a Nikon Optiphot™ light microscope using a 100x oil objective and a calibrated grid ocular.

Morphometric analysis

Tissue sections were scored blindly. Analyses were based on left cochleas, from which recordings were obtained. Quantitative assessment of cochleas focused on lateral wall and spiral limbus of the upper basal turn in a region expected to correspond to 10 kHz (±0.5 octave) (Ou et al., 2000b). This was done to avoid possible artifacts associated with electrode entry in the lower basal and apical turns and because changes in the upper base appeared typical of other locations. Metrics obtained depended upon whether a cochlea was taken for examination hours after noise (partially reversible cellular changes without cell loss), or weeks after noise (cell loss, other permanent pathology). Images taken for illustration were captured using a Diagnostic Instruments Model 1.4.0 digital camera controlled by Openlab^{TM} software, then further processed using Canvas^{TM}.

Acute noise injury (1–3 hrs after noise)—Quantitative assessment of acute noise injury (see Fig. 5) was based on a total of seven 3 month old CBA/J and CBA/CaJ mice, seven 2–4 month old B6 and B6.CAST mice, and seven 3–6 month old non-exposed controls for both groups. Measures were also obtained for 17 N2 backcross mice (see Fig. 13). Every fourth section was analyzed through a distance of 156 μm for a total 10 sections in each animal. Acute pathology was characterized non-parametrically using subjective judgments of ‘normal’ or ‘abnormal’ applied to stria vascularis, spiral ligament, and spiral limbus. Blind determination of normal/abnormal depended upon the clear presence of cell shrinkage, cell vacuolization, or the presence of void spaces between cells. For each structure, the number of sections scored abnormal was summed across animals within each experimental group. Noise-exposed mice of each strain were compared with non-exposed controls of the same strain by Z-test (Fig. 5), or tested for correlation with EP within animals by Pearson correlation (Fig. 13).

Permanent noise injury (8 wks after noise)—Quantitative assessment of permanent noise injury was based on a total of 6 CBA/J mice (3 mos at time of noise exposure) and 6 B6.CAST mice (3–4 mos at time of noise exposure. These were compared with six 3–6 month old non-exposed controls of each strain (see Figs. 7,8). Every fourth section was analyzed through a distance of 92 μm for a total 6 sections per animal. Permanent injury presents a combination of features that may be easily quantifiable (cell density), or less so (abnormal appearance of cells, void spaces between cells). A combination of parametric and non-parametric methods was therefore applied. Stria vascularis was blindly scored as ‘normal’ or ‘abnormal’ based on the presence of acellular material or void spaces between cells. Quantitative measures included strial thickness, strial marginal cell density, intermediate cell density, basal cell density, ligament thickness, density of Type I, II, and IV fibrocytes in the ligament, and density of fibrocytes in adjacent spiral limbus. Only nucleated profiles were included in cell counts. Strial thickness was measured orthogonal to the midpoint. Marginal cells, intermediate cells, and basal cells were counted in an 80 μm linear segment of stria, centered at the midpoint. No attempt was made to distinguish between lower and upper level intermediate cells, a distinction recently made by Schulte and Spicer (Spicer and Schulte, 2005). Ligament thickness was measured on an axis co-linear with the strial midline. Type I, II, and IV fibrocytes were counted in a 1,600 μm^2 area. These were identified based on location, an approach taken in previous studies (Hequembourg and Liberman, 2001;Lang et al., 2002;Hirose and Liberman, 2003). Fibrocytes in spiral limbus were counted in a roughly centered 1,600 μm^2 area, expected to be populated principally by stellate cells (Kimura et al.,

1990). For each metric, estimates from 6 sections were averaged to yield an overall average for each animal. Parametric data from noise-exposed animals were compared with non-exposed controls of the same strain by t-test (Figs. 7A,B, 8A,B). Nonparametric descriptors were converted to 'proportion abnormal' were compared between noise-exposed and non-exposed mice within each strain by Z-test (Figs. 7C, 8C)

Results

Control CAP threshold and EP

Abnormally elevated thresholds can reduce additional noise-induced hearing loss (Mills et al., 1997) and potential correlates such as EP reduction. To identify potential influences of initial pathology in any of our experimental groups, threshold and EP data were obtained from non-exposed controls. Figure 1 shows CAP thresholds (A) and EP in basal and apical turns (B) in control mice from each strain at the ages tested. Thresholds were tightly distributed within the expected normal range except for high frequency hearing loss in older B6 mice, as well as young albino and white-bellied agouti congenics. The modest hearing loss in the two congenic lines may reflect the fact that some of these mice were slightly older than the comparison young B6 mice (see Table I). Endocochlear potentials in the cochlear base and apex (Fig. 1B) were narrowly distributed across all strains, with the apex typically ~10 mV lower than the base.

Acute effects of noise on CBA and B6 threshold and EP

In the hours after noise exposure, few mice showed any CAP response above 10 kHz (not shown), regardless of strain. Figure 2A compares the effects of the noise on basal turn EP in B6 and CBA mice, measured in the hours after exposure. As reported by others (Wang et al., 2002; Hirose and Liberman, 2003), CBA/CaJ mice showed a 30–40 mV reduction. Significant reduction was also seen in CBA/J mice, and the reduction appeared independent of age at least up to 10 mos. By contrast, B6-related mice, which showed no significant change from control values. The lack of any impact of noise on the EP in B6 is independent of age up to 11 mos, and extends to the B6.CAST congenic line. Thus it appears independent of any direct or indirect effect of the *Cdh23*^{ahl} allele. Figure 2B also compares the EP in CBA and B6 mice after noise, but plots EP in the cochlear base versus apex. Normal EP values are expected to cluster to the right in the graph and to indicate ~10 mV higher values in the base (i.e., below the diagonal line). This expectation applies to the B6-related mice. CBA mice, however, show nearly complete separation from B6, and loss of the normal spatial EP gradient. Linear correlation indicates that the gradient actually reverses in the most severe cases.

Morphological correlates of acute EP changes

The sharp contrast in EP between CBA and B6 mice in the acute period after noise exposure showed clear anatomical correlates within the spiral ligament and stria vascularis. As illustrated in the cochlear upper basal turn of a single CBA/J mouse in Figure 3, these included shrinkage of Type I fibrocytes within the ligament (3A), vacuolization of strial basal cells (3A), and vacuolization of Type II fibrocytes in the ligament (3B). Such changes were largely absent from B6 mice, illustrated by example in a typical B6.CAST mouse in Figure 4 (upper basal turn). This animal shows a completely normal stria and Type I fibrocytes (4A), with delimited vacuolization of Type II fibrocytes (4B). Animals featured in Figures 3 and 4 were chosen to illustrate different types of acute pathology within the spiral limbus (Figs. 3C; 4C). Anomalies in limbus included both shrinkage of fibrocytes (Fig. 3C) and vacuolization of fibrocytes (Fig. 4C). Both types of pathology were observed in over 40% of noise-exposed animals of both strains. They also showed 20–30% incidence in controls, however, and thus did not reliably indicate strain differences or affects of noise in the hours after exposure.

Blind scoring of sections from CBA and B6 mice cochleas by light microscopy revealed marked quantitative strain differences in the hours after noise exposure, mirroring their difference in EP (Fig. 5). In CBA mice, the proportion of sections showing abnormalities of Type I fibrocytes (shrinkage), Type II fibrocytes (vacuolization), and stria vascularis (vacuolization of basal cells or other pathology) exhibited significant increases versus non-exposed controls (Fig. 5A). B6 mice showed significant increase only in the incidence of Type II fibrocyte pathology (Fig. 5B), and then only in ~30% of sections, compared to over 90% in CBAs.

Permanent effects of noise in CBA and B6 cochlea

Permanent effects of noise exposure on the CBA/CaJ mouse cochlea have been described in detail (Wang et al., 2002), thus it was of interest whether the qualitative differences seen acutely after noise in B6 and CBA mice have analogs in permanent injury. At 8 wks post-exposure, thresholds had recovered at lower frequencies in CBA/J, but showed much less recovery in B6.CAST (Fig. 6A). This is consistent with previous studies showing greater noise vulnerability in B6 mice (Erway et al., 1993; Erway et al., 1996; Johnson et al., 1997; Davis et al., 2001), even when *Cdh23*^{ahl} is removed from the genetic background (Ortmann et al., 2004). By contrast with thresholds, the EP showed essentially complete recovery in both strains (Fig. 6B).

The cellular targets of noise exposure during the acute phase in CBA/J mice had reliable analogs at 8 wks post noise. CBA/J mice showed statistically significant loss of Type I and II fibrocytes and strial basal cells (Fig. 7A). Subtle losses of fibrocytes were not attended by obvious visual differences under the light microscope (see Fig. 3D,E). Although no significant loss of strial cell types other than basal cells was detected (Fig. 7A), there was modest loss of strial capillaries not predicted by any observations in the acute phase. Permanent injury was also found in spiral limbus, wherein the central zone was rendered almost completely acellular (Fig. 7A; see example in Fig. 3F).

The most glaring permanent defect in the cochlear lateral wall of CBAs was the general appearance of the stria (see Fig. 3D). Extracellular void spaces and non-cellular debris were found in nearly 90% of sections scored (Fig. 7C). Often the location of voids corresponded to the expected location of a capillary. Both spiral ligament and stria vascularis became significantly thinner in CBA/J (Fig. 7B), perhaps as a result of basal cell and capillary loss.

None of the cell loss and other pathology found to be significant in CBA/J mice was significant in B6.CAST mice (Fig. 8). The only trend suggested was highly variable thinning of the spiral ligament (Fig. 8B). As in CBA/J, visual inspection of B6.CAST ligament revealed no obvious anomalies (see Fig, 4D,E). By contrast with CBAs, however, B6.CAST stria and limbus also appeared normal (Fig. 4D,F). The incidence of strial abnormalities of any kind in B6.CAST was no greater than that observed in controls (Fig. 8C).

Testing the role of melanin-related genes

As an initial approach to genetic analysis of the differences between B6 and CBA mice, we considered the possible role of melanin and genes related to melanin production. Melanin is produced by melanocytes, including strial intermediate cells. Eumelanin, the predominant form in B6 mice, is suggested to be protective against cochlear injury (Conlee et al., 1988; Barrenas and Lindgren, 1991; Barrenas, 1997), and alpha melanocyte stimulating hormone (αMSH), which partly mediates the production of eumelanin, may have additional protective effects within the cochlea (Hamers et al., 2002; Wolters et al., 2003). Unlike B6 mice, CBA mice carry the dominant agouti trait (*A*) and may produce the agouti protein within the cochlea. Agouti protein antagonizes αMSH, thereby promoting production of pheomelanin (Voisey and Van

Daal, 2002), which may be ototoxic (Barrenas and Holgers, 2000). CBA mice may therefore be subject to harmful actions of cochlear pheomelanin, and also lack any benefits of eumelanin or αMSH. Because of the availability of co-isogenic lines to B6 that either do not make melanin (C57BL/6-*Tyr*$^{c\text{-}2J}$, albino), or make pheomelanin (C57BL/6J-*A*$^{w\text{-}J}$, white-bellied agouti), we could explicitly examine the possible role of melanin in our strain results. While the *A*$^{w\text{-}J}$ allele is different from the *A* allele carried by CBA, it is believed to represent the wild type agouti allele (Sandulache et al., 1994) and to be at least as widely expressed as the *A* allele and exert similar effects. Figure 9 shows CAP thresholds (A) and EP results (B) for the two congenic models 1–3 hrs after noise exposure. Acute threshold shifts for the albinos were similar to those in the B6 parent strain. These mice exhibited a modest (~10 mV) but significant reduction in both basal and apical turn EP in the acute phase. This reduction was not associated with any anatomical changes detectable by light microscope (not shown). The white-bellied agouti mice showed surprisingly little threshold shift after noise (Fig. 9A) and no significant EP reduction (B). In summary, neither the elimination of melanin nor its replacement with an alternate form substantively reproduce our CBA results nor convert B6 mice into a CBA noise phenotype.

Inheritance pattern of noise injury in F1 and N2 backcross mice

The inheritance mode of the CBA noise phenotype was examined in CBAxB6 F1 hybrid mice. Like both parent strains, most F1s exhibited no CAP response above 10 kHz in the acute phase after noise exposure (not shown). However, they showed acute EP reduction that was statistically indistinguishable (t-test, p=0.12) from that seen in the CBA parent strain (compare Figs. 10,2). The pattern of acute cellular pathology also appeared identical to that in the CBA/J parent strain. Figure 11A shows a typical F1 animal with severe EP reduction and CBA-characteristic pathology including vacuolization of strial basal cells and Type II fibrocytes, as well as shrinkage of Type I's. No gender effect was evident. These results suggested that the CBA noise phenotype is inherited in an autosomal dominant manner and that all aspects of the phenotype are 'co-inherited' as part of a single injury cascade impacted by just one or a few loci.

Examination of the distribution of a quantitative phenotype in backcross mice is a typical method for inferring the number of loci that play a prominent role, and for mapping those loci. Suspecting we were dealing with one or a few dominant alleles, we examined 42 [(B6.CASTxCBA F1) x B6.CAST] N2 backcross mice. Progeny from such a cross can be homozygous only for B6 alleles, while half are expected to carry a CBA allele at any locus. We thus expected that if our trait of interest was dominated by one or a few quantitative trait loci (QTLs), the distribution of phenotypes among N2 mice should fall into 2–3 clear modes. Figure 12 shows the physiological results for the N2 progeny 1–3 hrs after noise exposure. Unlike either parent strain or their F1 hybrid, several N2 mice still showed CAP responses at the highest test frequencies. At 28.3 kHz, for example, 26 of 42 mice tested had no detectable response, while the remaining 16 mice showed responses with thresholds as low as 60 dB SPL. For the latter, there was a significant correlation between basal turn EP and CAP threshold (Fig. 12A), having a slope of −0.44 dB/mV. Thus, in individuals not rendered completely unresponsive by noise (presumably due to assortment of unknown alleles governing noise susceptibility of the organ of Corti), EP reduction can modulate hearing thresholds.

Comparison of basal and apical turn EP in N2 mice recapitulated the relation seen in the inbred strains (Fig. 2B), whereby near-normal basal EPs were associated with apical turn EPs that were ~10 mV lower, and very low EPs were associated with reversal of the normal basal-apical gradient (Fig. 12B).

EP values obtained for N2 mice during the acute phase were not normally distributed (Kolmogorov-Smirnov, p=0.007). Matching expectations for a trait dominated by a single dominant-acting major effect QTL, basal turn EPs were well fit by two Gaussians, a narrowly-

distributed 'normal EP' population (mean ± SD 103.5 ± 6.3 mV) and a more broadly distributed 'depressed EP' population (64.3 ± 14.1 mV) (Fig. 12C). Of the 42 noise-exposed N2 mice, 21 had an EP above 90 mV, and 21 had an EP below 90 mV, supporting two highly penetrant genotypes inherited with equal chance. Two-way ANOVA showed no effect of gender or coat color. Using the variance in basal turn EP pooled across all exposed and non-exposed B6 and B6.CAST mice (n=38; s^2=40.7) to estimate non-genetic variation, and the variance of the EP in exposed N2 mice to estimate genetic variation (n=42; s^2=509.6), we calculated that 86% of the variation in EP after noise exposure in the N2 mice was inherited (Hegmann and Possidente, 1981).

Variation in the effects of noise among N2 mice provided an opportunity to test the possibility of 'co-inheritance' of all facets of the CBA noise phenotype. Figure 11B and C show typical examples. The N2 animal depicted in Figure 11B exhibited marked EP reduction and shows CBA-characteristic pathology of spiral ligament and stria. The animal in Figure 11C had a normal EP and showed no evidence of acute cellular pathology. If pathology of stria and ligament do reliably co-occur, the probability of pathology of these structures should ideally be correlated with endocochlear potential in the N2 mice. Figure 13 shows that this was indeed the case. In the acute phase after noise, the proportion of sections in which the stria was judged 'normal' correlated well with the EP (A). Even subtle pathology of Type I and Type II fibrocytes was well correlated with the EP (Fig. 13B,C), supporting the contention that these characteristics have a common basis.

Acute clues to permanent anatomical changes

Anomalies of Type I and II fibrocytes and strial basal cells were observed both 1–3 hrs and 8 wks after noise exposure in CBA mice. Early injury was therefore a good predictor of some permanent cell loss CBAs. Neither strial capillary loss nor loss of fibrocytes from spiral limbus, however, was presaged by changes evident by light microscope at 1–3 hrs. As others have emphasized (Duvall et al., 1974; Ide and Morimitsu, 1990; Wang et al., 2002; Hirose and Liberman, 2003), the appearance of the cochlear lateral wall can change dramatically in the hours and days after noise exposure. The finding of a similar pattern of acute pathology in CBAs, B6/CBA F1 hybrids, and N2 backcross mice with EP reduction suggests that all these would appear similar at other time points as well. To better understand the relation between the acute and permanent pathology characteristic of CBA mice, we examined F1 hybrid mice taken for examination at 24 hrs post-noise. At this time, each of 8 mice tested showed responses to high frequency stimuli, albeit with greatly elevated thresholds, and three mice exhibited basal turn EPs greater than 80 mV (not shown), indicating partial recovery of both organ of Corti and the lateral wall. Consistent with previous reports, animals showing a depressed EP at 24 hrs also exhibited marked strial swelling associated expansion of the intra-strial space (Fig. 14A). Vacuole formation within cells, as seen 1–3 hrs after noise in basal cells, was uncommon. Few examples of moribund strial cells (pyknotic nuclei, darkened cytoplasm) were seen, nor were any signs of injury to capillaries apparent. However, nearly all sections revealed signs of impending cell death in both spiral ligament and limbus. As illustrated in Figure 14, most sections included multiple examples of Type I and II fibrocytes (14A) and limbus fibrocytes (14B) with condensed nuclei. Type I fibrocytes often showed darkened cytoplasm and appeared shrunken, leaving void spaces in the surrounding extracellular matrix. Obvious pathology of the limbus typically appeared only in the apical turn, suggesting an apical-to-basal progression that has not reached the basal turn by 24 hrs. Thus, with the exception of capillary loss, when the observation window is extended to 24 hrs post-exposure, clear signs of all permanent injury noted in CBA mice at 8 wks can be found. Finding of these signs in F1 mice further supports the contention that all aspects of the CBA noise injury phenotype (loss of cells in stria, ligament, and limbus) are causally related.

Since the F1 mice examined at 24 hrs showed CAP responses at high frequencies, it was possible to repeat the analysis described earlier for the N2 mice, examining the relation between the basal turn EP and CAP response thresholds. CAP thresholds at 20 kHz were significantly correlated with the EP (R^2=0.74; p<0.001) (not shown). The slope of the relation was −0.36 dB/mV. The N2 and F1 results are therefore in rough agreement, indicating that noise-related depression of the EP can influence hearing thresholds, given the right genetic background.

Discussion

To date, mapping of hearing-related genes in mice has relied entirely on distributions of hearing thresholds e.g.,(Johnson et al., 2006). Here we report a surprisingly robust phenotype revealed only by noise exposure that is manifested through the EP rather than threshold, and is closely tied to a set of well delineated pathologies of cochlear lateral wall and spiral limbus. These appear to share a 'co-inherited' predisposition, either because all affected cells express the underlying gene, or (more likely) because all affected cells participate in the same impaired process. Based on our results, cochlear noise injury may not possess just one archetype even within a species, and the genes that modulate injury may act independently on different cells and structures. In the case of CBA and B6 mice, noise vulnerability of the organ of Corti and lateral wall/limbus appear subject to different genetic influences, with potentially very different impact on further changes over time.

A significant economy we employed was reliance on a single cochlear location for our histological measures. This was successful because of the representative nature of the cochlear upper base, and because all experimental groups were analyzed equivalently. Among key metrics, only those characterizing the spiral limbus appeared subject to spatial bias, in that the earliest detected anomalies of the limbus appeared in the lower apical turn, not the upper base (Fig. 14). We previously used a single location approach to demonstrate mouse strain differences in age-related pathology of the cochlear lateral wall (Ohlemiller et al., 2006).

We cannot be certain regarding the range of noise exposure conditions over which our findings would apply. Parametric studies in guinea pigs and chinchillas support a single major inflection in the relation between noise intensity and the nature of cochlear injury (Spoendlin and Brun, 1973; Ward and Turner, 1982; Fredelius et al., 1987). As exposure levels approach 125–130 dB SPL, there occurs a transition from predominantly metabolic injury (injury proceeding from unmet energy demands) to traumatic injury (direct mechanical trauma). Above this level the reticular lamina may fracture, eliminating the boundary between perilymphatic and endolymphatic spaces. As a result, cells of the organ of Corti are exposed to toxic levels of potassium (Bohne and Rabbit, 1983) and the input resistance of scala media plummets, along with the EP. Although the transition from metabolic to traumatic injury may occur at a relatively low noise intensity in mice (116 dB SPL) (Wang et al., 2002; Hirose et al., 2005), we found no evidence for a breach in the integrity of scala media. The previous studies in CBA/CaJ mice suggest that the types of injury we describe in stria vascularis of CBA mice can occur over a wide range of noise intensities (94–112 dB SPL). Since we operated at the upper end of this range, for our results to simply reflect an injury threshold difference between CBA and B6 mice would require an implausibly large difference.

Noise injury in the cochlear lateral wall and spiral limbus

Of many previous studies of noise injury to the cochlear lateral wall in animals e.g.,(Ward and Duvall, 1971; Johnsson and Hawkins, 1972; Duvall et al., 1974; Santi and Duvall, 1978; Ulehlova, 1983; Ide and Morimitsu, 1990), few have been quantitative or included recording of the EP. Most of these indicate that significant permanent strial injury requires extreme exposure conditions, but have left unresolved the question of when strial injury contributes to permanent hearing loss. Our acute and permanent noise injury findings in CBA/J and CBA/

CaJ are consistent with the previous reports in CBA/CaJ (Wang et al., 2002; Hirose and Liberman, 2003), although those mentioned neither acute nor permanent pathology of Type I fibrocytes or strial basal cells, and strial capillary loss was not noted. While not emphasized here, we also confirmed earlier findings of injury and loss of Type IV fibrocytes in spiral ligament see also(Hirose et al., 2005). CBA and B6 mice showed similar effects of noise on these cells.

In mice and other models (Duvall et al., 1974; Ide and Morimitsu, 1990; Wang et al., 2002; Hirose and Liberman, 2003), the appearance of the lateral wall, and especially the stria, can vary markedly in the hours and days after noise. Upon viewing the dramatic swelling of the stria that occurs ~24 hrs after noise (e.g., Fig. 14), one might expect the stria to undergo obvious cell loss. Yet although the stria ultimately becomes markedly thinner, shows many void spaces, and appears less well organized (Figs. 3D, 7), only modest loss of basal cells and capillaries was observed. Most significantly, the EP returns to normal values, so that changes in the stria presumably do not impact hearing thresholds. It remains to be determined, however, whether the long term stability and apparent aging characteristics of the stria are affected.

The pathology evident within the first day after noise in CBA mice was a good indicator of eventual permanent injury to stria, spiral ligament, and limbus. Type I and Type II fibrocytes appeared abnormal in the hours after noise, and at 24 hrs were clearly in the process of degenerating (Fig. 14A). At 8 wks, they were significantly reduced in number. Strial basal cells, the only strial cells obviously affected immediately after noise, were also significantly reduced in number at 8 wks. Dramatic loss of fibrocytes from spiral limbus in the cochlear upper base at 8 wks was not presaged by consistent acute pathology at that location. However, marked pathology of the limbus appeared more apically by 24 hrs (Fig. 14B), suggesting that noise injury to the limbus begins apically and progresses toward the base, as may also occur in aging (Ohlemiller and Gagnon, 2004). Of all permanent injury to stria we identified, only strial capillary loss gave no acute sign at the level of the light microscope.

The loss of ligament fibrocytes and strial basal cells measured 8 wks post-exposure in CBA mice was modest. At 24 hrs, however, the number of abnormal-appearing ligament versus strial cells was quite different: While nearly every section examined showed pyknotic fibrocytes in spiral ligament, abnormal-appearing basal or other strial cells were rare. Lest this seem a contradiction, strial swelling was marked by expanded extracellular space and not by large intracellular vacuoles or abnormal-appearing cell nuclei, as if the swelling is adaptive rather than destructive. The apparent discrepancy between the seemingly higher initial rate of loss of fibrocytes than basal cells and their modest differences at 8 wks may be attributable to different rates of cell replacement, which appears more rapid in the ligament than in the stria (Lang et al., 2003; Yamasoba et al., 2003).

Contribution of the EP to hearing loss and noise susceptibility

The present and previous results in CBA mice demonstrate that EP reduction can participate in hearing loss in the acute injury phase after noise. The slope of this relation for CAP thresholds at high frequencies is about −0.4 dB/mV, the value that emerged from independent estimates in F1 and N2 mice. This value is smaller than that derived from experiments wherein the EP was pharmacologically reduced (−1 dB/mV) (Sewell, 1984; Schmiedt et al., 2002). Although EP reduction has thus far only been found under exposure conditions that lead to permanent hearing loss, there may be exposure conditions or models wherein EP reduction significantly modulates purely temporary hearing loss. Our results further make it clear that participation of the EP in the acute phase of hearing loss depends on genetic makeup. Since EP depression can reduce permanent noise-induced hearing loss (Kanno et al., 1993), our results may help explain variation in noise susceptibility in among mouse strains and perhaps among humans.

Mechanisms of noise-related pathology

The stria vascularis generates part of the electrochemical potential supporting ion currents through cochlear hair cells (Wangemann and Schacht, 1996). Two distinct functions of the stria, generation of the EP and creation of a high potassium concentration in endolymph, appear localizable to distinct compartments within the stria (Salt et al., 1987; Spicer and Schulte, 2005). The spiral limbus is also believed to contribute to maintenance of high K+ levels in endolymph (Spicer and Schulte, 1998). Potassium pumping functions of the stria and limbus rely upon Na+/K+-ATPase in strial marginal cells and limbal interdental cells, respectively. These cells may become energetically taxed during noise exposure, impairing K+ flux through stria and limbus and promoting K+ buildup along proposed medial and lateral 'recycling' routes that guide K+ from the organ of Corti back to scala media (Spicer and Schulte, 1998; Wangemann, 2002). The posited routes encompass a syncytium of connected supporting cells and fibrocytes, so that the principle flow occurs within cells. If ion flux through stria and limbus becomes acutely impaired, accumulation of excess K+ 'upstream' would be expected to promote osmotic imbalance and fluid influx into the cells composing the network, resulting in vacuolization and possible injury. Cells that might show such effects prominently include all fibrocytes of the spiral ligament and limbus, but not necessarily marginal cells or interdental cells themselves. The notion of an upstream K+ buildup does not readily explain why the specific form of pathology differed for Type II fibrocytes (which appeared vacuolized) and Type I fibrocytes (which appeared shrunken). This pattern suggests that ion accumulation occurred within the Type II's, but outside the Type I's. One possibility is that noise disrupts claudin tight junctions between strial basal cells that normally prevent K+ from flowing from the stria back to the ligament (Gow et al., 2004). It is also not clear why obvious acute strial pathology would emphasize basal cells, given that these are thought to be electrotonically linked to Type I fibrocytes, strial intermediate cells, and strial capillary pericytes and endothelial cells (Spicer and Schulte, 1998; Tacheuchi et al., 2000). Noise may promote electrical isolation of these cells (Todt et al., 1999), perhaps even as part of a compensatory mechanism.

Among cochlear structures, the stria is particularly sensitive to metabolic poisons (Yamasoba et al., 2006) and transient cochlear ischemia (Morizane et al., 2005). Although these typically impose greater injury than did our noise exposure, modest energy manipulations can reproduce many of our observations. Round window application of 50 μM 3-nitropropionic acid, a mitochondrial inhibitor, to guinea pigs (Hoya et al., 2004; Okamoto et al., 2005) yields reversible pathology of spiral ligament, stria vascularis, and spiral limbus with remarkable similarities the effects of noise in CBA mice, including strial injury that is restricted to vacuolation of strial basal cells (not noted by the authors). Such effects are consistent with a noise-inflicted 'energy crisis' in cells having major K+ pumping functions, most other injury being secondary. The crisis may be exacerbated by reduction in cochlear blood flow mediated by oxidative stress (Hawkins, 1971; Yamane et al., 1995; Miller et al., 2003).

Genetic basis of strain differences

Based on the distribution of EPs in the acute injury phase in our F1 and N2 mice, the CBA noise phenotype may be established by as few as one autosomal dominant-acting major effect QTL. From the preceding arguments, the affected gene product may be one involved in energy production or utilization, or could modulate cochlear blood flow. Other possibilities, such as an ion channel or pump, cannot be discounted.

Based on comparison of mice carrying different alleles encoding Cdh23, agouti protein and tyrosinase, major roles for these as a basis for our strain results are unlikely. Our investigation of the role of melanin was predicated on suggested protective effects of eumelanin (found in B6), possible harmful effects of alternate forms (as in CBA), and inhibition of αMSH by the

agouti protein (as in CBA) (Meyer zum Gottesberge, 1988; Barrenas and Lindgren, 1991; Wolters et al., 2003). The significance of the amount and form of cochlear melanin was tested using co-isogenic lines to B6. White bellied agouti B6 showed no EP reduction after noise, arguing against any general effect of alternate melanin forms or inhibition of αMSH. They also showed surprising noise resistance (Fig. 9). 129S6/SvEv mice, which are resistant to noise (Yoshida et al., 2000), also carry the $A^{w\text{-}J}$ allele, so that this allele may impart noise protection to both strains. Albino B6 mice exhibited modest but significant EP reduction hours after noise. Thus complete absence of melanin may render the stria more vulnerable to noise injury. We could find no anatomical correlate to the modest EP reduction, however, and this result does not account for our B6 versus CBA differences.

Acknowledgements

Supported by NIH R01 DC03454 (K.K. Ohlemiller), P30 DC04665 (D.D. Simmons), and Washington University Med. School Dept. of Otolaryngology. Thanks to Drs. K.P. Steel and K.R. Johnson for advice on informative mouse strains and to J. Lett, J. Bark, and T. Rogers for technical assistance.

References

Axelsson A, Borg E, Hornstrand C. Noise effects on the cochlear vasculature in normotensive and spontaneously hypertensive rats. Acta Otolaryngol 1983;96:215–225. [PubMed: 6637443]

Barrenas ML, Holgers KM. Ototoxic interaction between noise and pheomelanin: Distortion product otoacoustic emissions after acoustical trauma in chloroquine-treated red, black, and albino guinea pigs. Audiology 2000;39:238–246. [PubMed: 11093607]

Barrenas ML, Lindgren F. The influence of eye color on susceptibility to TTS in humans. Br J Audiol 1991;25:303–307. [PubMed: 1742556]

Barrenas M. Hair cell loss from acoustic trauma in chloroquine-treated red, black and albino guinea pigs. Audiology 1997;36:187–201. [PubMed: 9253479]

Beagley HA. Acoustic trauma in the guinea pig. I Electrophysiology and Histology. Acta Otolaryngol 1965;60:437–451.

Bohne BA, Rabbit KD. Holes in the reticular lamina after noise exposure: Implications for continued damage in the organ of Corti. Hearing Res 1983;11:41–53.

Borg E. Noise-induced hearing loss in normotensive and spontaneously hypertensive rats. Hear Res 1982;8:117–130. [PubMed: 7142039]

Borg E, Canlon B, Engstrom B. Noise-induced hearing loss: Literature review and experiments in rabbits. Morphological and physiological features, exposure parameters and temporal factors, variability and interactions. Scand Audiol (Suppl) 1995;40:1–147. [PubMed: 7732328]

Candreia C, Martin GK, Stagner BB, Lonsbury-Martin BL. Distortion product otoacoustic emissions show exceptional resistance to noise exposure in MOLF/Ei mice. Hear Res 2004;194:109–117. [PubMed: 15276682]

Conlee JW, Abdul-Baqi KJ, McCandless GA, Creel DJ. Effects of aging on normal hearing loss and noise-induced threshold shift in albino and pigmented guinea pigs. Acta Otolaryngol 1988;106:64–70. [PubMed: 3421100]

Covell WP. Histologic changes in the organ of Corti with intense sound. J Comp Neurol 1953;99:43–59. [PubMed: 13084782]

Davis RR, Kozel P, Erway LC. Genetic influences in individual susceptibility to noise: a review. Noise and Health 2003;5:19–28. [PubMed: 14558889]

Davis RR, Newlander JK, Ling XB, Cortopassi GA, Kreig EF, Erway LC. Genetic basis for susceptibility to noise-induced hearing loss in mice. Hear Res 2001;155:82–90. [PubMed: 11335078]

Duvall AJ, Ward WD, Lauhala KE. Stria ultrastructure and vessel transport in acoustic trauma. Ann Otol 1974;83:498–514.

Erway LC, Shiau YW, Davis RR, Kreig EF. Genetics of age-related hearing loss in mice. III Susceptibility of inbred and F1 hybrid strains to noise-induced hearing loss. Hear Res 1996;93:181–187. [PubMed: 8735078]

Erway LC, Willott JF, Archer Jr, Harrison DE. Genetics of age-related hearing loss in mice: I. Inbred and F1 hybrid strains. Hear Res 1993;65:125–132. [PubMed: 8458745]

Fredelius L, Johansson B, Bagger-Sjoback D, Wersall J. Qualitative and quantitative changes in the guinea pig organ of Corti after pure tone acoustic overstimulation. Hear Res 1987;30:157–168. [PubMed: 3680063]

Gow A, Davies C, Southwood CM, Frolenkov G, Chrustowski M, Ng L, Yamauchi D, Marcus DC, Kachar B. Deafness in *claudin 11*-null mice reveals the critical contribution of basal cell tight junctions to stria vascularis function. J Neurosci 2004;24:7051–7062. [PubMed: 15306639]

Hamernik RP, Patterson JH, Turrentine GA, Ahroon WA. The quantitative relation between sensory cell loss and hearing thresholds. Hear Res 1989;38:199–212. [PubMed: 2708163]

Hamers FPT, Wijbenga J, Wolters FLC, Klis SFL, Sluyter S, Smoorenburg GF. Cisplatin ototoxicity involves organ of Corti, stria vascularis and spiral ganglion: modulation by α MSH and ORG 2766. Audiol NeuroOtol 2002;8:305–315. [PubMed: 14566101]

Harding GW, Baggot PJ, Bohne BA. Height changes in the organ of Corti following noise exposure. Hear Res 1992;63:26–36. [PubMed: 1464572]

Hawkins JE. The role of vasoconstriction in noise-induced hearing loss. Annals Otol Rhinol Laryngol 1971;80:903–913.

Hegmann JP, Possidente B. Estimating genetic correlations from inbred strains. Behav Genet 1981;11:103–114. [PubMed: 7271677]

Henry KR. Influence of genotype and age on noise-induced auditory losses. Behav Gen 1982;12:563–573.

Hequembourg S, Liberman MC. Spiral ligament pathology: A major aspect of age-related cochlear degeneration in C57BL/6 mice. J Assoc Res Otolaryngol 2001;2:118–129. [PubMed: 11550522]

Hirose K, Discolo CM, Keasler JR, Ransohoff R. Mononuclear phagocytes migrate into the murine cochlea after acoustic trauma. J Comp Neurol 2005;489:180–194. [PubMed: 15983998]

Hirose K, Liberman MC. Lateral wall histopathology and endocochlear potential in the noise-damaged mouse cochlea. J Assoc Res Otolaryngol 2003;4:339–352. [PubMed: 14690052]

Hoya N, Okamoto Y, Kamiya K, Fujii M, Matsunaga T. A novel animal model of acute cochlear mitochondrial dysfunction. Neuroreport 2004;15:1597–1600. [PubMed: 15232290]

Ide M, Morimitsu T. Long term effects of intense sound on endocochlear DC potential. Auris Nasus Larynx 1990;17:1–10. [PubMed: 2390027]

Johnson KR, Erway LC, Cook SA, Willott JF, Zheng QY. A major gene affecting age-related hearing loss in C57BL/6J mice. Hear Res 1997;114:83–92. [PubMed: 9447922]

Johnson KR, Zheng QY, Noben-Trauth K. Strain background effects and genetic modifiers of hearing in mice. Brain Res 2006;1091:79–88. [PubMed: 16579977]

Johnson LG, Hawkins JE. Degeneration patterns in human ears exposed to noise. Ann Otol 1976;85:725–739.

Johnsson LG, Hawkins JE. Strial atrophy in clinical and experimental deafness. Laryngoscope 1972;82:1105–1125. [PubMed: 5078636]

Kanno H, Ohtani I, Hara A, Kusakari J. The effect of endocochlear potential suppression upon susceptibility to acoustic trauma. Acta Otolaryngol 1993;113:26–30. [PubMed: 8442418]

Kimura RS, Nye CL, Southard RE. Normal and pathologic features of the limbus spiralis and its functional significance. Am J Otolaryngol 1990;11:99–111. [PubMed: 2344002]

Kozel PJ, Davis RR, Kreig EF, Schull GE, Erway LC. Deficiency in plasma membrane calcium ATPase isoform 2 increases susceptibility to noise-induced hearing loss in mice. Hear Res 2002;164:231–239. [PubMed: 11950541]

Lang H, Schulte BA, Schmiedt RA. Endocochlear potentials and compound action potential recovery: functions in the C57BL/6J mouse. Hear Res 2002;172:118–126. [PubMed: 12361874]

Lang H, Schulte BA, Schmiedt RA. Effects of chronic furosemide treatment and age on cell division in the adult gerbil inner ear. J Assoc Res Otolaryngol 2003;4:164–175. [PubMed: 12943371]

Li HS. Influence of genotype and age on acute acoustic trauma and recovery in CBA/Ca and C57BL/6J mice. Acta Otolaryngol 1992;112:956–967. [PubMed: 1481666]

Liberman MC, Dodds LW. Single neuron labeling and chronic cochlear pathology. III Stereocilia damage and alterations of threshold tuning curves. Hear Res 1984;16:55–74. [PubMed: 6511673]

Liberman MC, Kiang NYS. Acoustic trauma in cats: Cochlear pathology and auditory nerve activity. Acta Otolaryngol 1978;358:1–63.

Liberman, MC.; Mulroy, MJ. Acute and chronic effects of acoustic trauma: Cochlear pathology and auditory nerve pathophysiology. In: Hamernik, RP.; Henderson, D.; Salvi, R., editors. New Perspectives on Noise-induced Hearing Loss. Raven Press; New York: 1982. p. 105-135.

Meyer zum Gottesberge AM. Physiology and pathophysiology of inner ear melanin. Pig Cell Res 1988;1:238–249.

Miller JM, Brown JN, Schacht J. 8-iso-prostglandin F(2alpha), a product of noise exposure, reduces inner ear blood flow. Audiol Neuro-Otol 2003;8:207–221.

Mills JH, Boettcher FA, Dubno JR. Interaction of noise-induced permanent threshold shift and age-related threshold shift. J Acoust Soc Am 1997;101:1681–1686. [PubMed: 9069635]

Morizane I, Hakuba N, Shimizu Y, Shinomori Y, Fujita K, Yoshida T, Shudou M, Gyo K. Transient cochlear ischemia and its effects on the stria vascularis. Neuroreport 2005;16:799–802. [PubMed: 15891573]

Nordmann AS, Bohne BA, Harding GW. Histopathological differences between temporary and permanent threshold shift. Hear Res 2000;139:13–30. [PubMed: 10601709]

Ohlemiller KK, Gagnon PM. Apical-to-basal gradients in age-related cochlear degeneration and their relationship to 'primary' loss of cochlear neurons. J Comp Neurol 2004;479:103–116. [PubMed: 15389608]

Ohlemiller KK, Lett JM, Gagnon PM. Cellular correlates of age-related endocochlear potential reduction in a mouse model. Hear Res 2006;220:10–26. [PubMed: 16901664]

Ohlemiller KK, McFadden SL, Ding DL, Lear PM, Ho YS. Targeted mutation of the gene for cellular glutathione peroxidase (*Gpx1*) increases noise-induced hearing loss in mice. J Assoc Res Otolaryngol 2000;1:243–254. [PubMed: 11545230]

Ohlemiller KK, McFadden SL, Ding DL, Reaume AG, Hoffman EK, Scott RW, Wright JS, Putcha GV, Salvi RJ. Targeted deletion of the cytosolic Cu/Zn-Superoxide Dismutase gene (SOD1) increases susceptibility to noise-induced hearing loss. Audiol Neuro-Otol 1999;4:237–246.

Ohlemiller KK, Patel PR, Lear PM. The endocochlear potential (EP) in C57BL/6 mice is resistant to noise exposure. Abstr Assoc Res Otolaryngol 2003;26:268.

Okamoto Y, Hoya N, Kamiya K, Fujii M, Ogawa K, Matsunaga T. Permanent threshold shifts caused by acute cochlear mitochondrial dysfunction is primarily mediated by degeneration of the lateral wall of the cochlea. Audiol NeuroOtol 2005;10:220–233. [PubMed: 15809501]

Ortmann AJ, Faulkner KF, Gagnon PM, Ohlemiller KK. Removal of the Ahl allele from the C57BL/6 background does not improve noise resistance. Abstr Assoc Res Otolaryngol 2004;27:168.

Ou HC, Bohne BA, Harding GW. Noise damage in the C57BL/CBA mouse cochlea. Hear Res 2000a; 145:111–122. [PubMed: 10867283]

Ou HC, Harding GW, Bohne BA. An anatomically based frequency-place map for the mouse cochlea. Hear Res 2000b;145:123–129. [PubMed: 10867284]

Puel JL, Ruel J, Gervais d'Aldin C, Pujol R. Excitotoxicity and repair of cochlear synapses after noise-trauma induced hearing loss. NeuroRep 1998;9:2109–2114.

Robertson D. Functional significance of dendritic swelling after loud sounds in the guinea pig cochlea. Hear Res 1983;9:263–278. [PubMed: 6841283]

Salt AN, Melichar I, Thalmann R. Mechanisms of endocochlear potential production by stria vascularis. Laryngoscope 1987;97:984–991. [PubMed: 3613802]

Salvi, R.; Perry, J.; Hamernik, RP.; Henderson, D. Relationships between cochlear pathologies and auditory nerve and behavioral responses following acoustic trauma. In: Hamernik, RP.; Henderson, D.; Salvi, R., editors. New Perspectives in Noise-induced Hearing Loss. Raven Press; New York: 1982. p. 165-188.

Sandulache R, Neuhauser-Klaus A, Favor J. Genetic instability at the *agouti l*ocus of the mouse (*Mus musculus*) I Increased reverse mutation frequency to the A^w allele in *A/a* heterozygotes . Genetics 1994;137:1079–1087. [PubMed: 7982562]

Santi PA, Duvall AJ. Stria vascularis pathology and recovery following noise exposure. Otolaryngology-Head and Neck Surgery 1978;86:354–361.

Saunders JC, Cohen YE, Szymko YM. The structural and functional consequences of acoustic injury in the cochlea and peripheral auditory system. J Acoust Soc Am 1991;90:136–146. [PubMed: 1880281]

Saunders, JC.; Tilney, LG. Species differences in susceptibility to noise exposure. In: Hamernik, RP.; Henderson, D.; Salvi, R., editors. New Perspectives on Noise-Induced Hearing Loss. Raven Press; New York: 1980. p. 229-248.

Schmiedt RA, Lang H, Okamura H, Schulte BA. Effects of furosemide applied chronically to the round window: A model of metabolic presbycusis. J Neurosci 2002;22:9643–9650. [PubMed: 12417690]

Sewell W. The effects of furosemide on the endocochlear potential and auditory nerve fiber tuning curves in cats. Hear Res 1984;14:305–314. [PubMed: 6480516]

Slepecky N. Overview of mechanical damage to the inner ear: noise as a tool to probe cochlear function. Hear Res 1986;22:307–321. [PubMed: 3090001]

Spicer SS, Schulte BA. Evidence for a medial K+ recycling pathway from inner hair cells. Hear Res 1998;118:1–12. [PubMed: 9606057]

Spicer SS, Schulte BA. Novel structures in marginal and intermediate cells presumably relate to functions of basal versus apical strata. Hear Res 2005;200:87–101. [PubMed: 15668041]

Spoendlin H, Brun JP. Relation of structural damage to exposure time and intensity in acoustic trauma. Acta Otolaryngol 1973;75:220–226. [PubMed: 4571032]

Syka J, Melichar I, Ulehlova L. Longitudinal distribution of cochlear potentials and the K+ concentration in the endolymph after acoustic trauma. Hear Res 1981;4:287–298. [PubMed: 7263516]

Tacheuchi S, Ando M, Kakigi A. Mechanism generating endocochlear potential: Role played by intermediate cells in stria vascularis. Biophys J 2000;79:2572–2582. [PubMed: 11053131]

Todt I, Ngezahayo A, Ernst A, Kolb HA. Inhibition of gap junctional coupling in cochlear supporting cells by gentamicin. Pflug Arch Eur J Physiol 1999;438:865–867.

Ulehlova L. Stria vascularis in acoustic trauma. Arch Otorhinolaryngol 1983;237:133–138. [PubMed: 6847511]

Vazquez AE, Jimenez AM, Martin GK, Luebke AE, Lonsbury-Martin BL. Evaluating cochlear function and the effects of noise exposure in the B6. CAST+Ahl mouse with distortion product otoacoustic emissions. Hear Res 2004;194:87–96. [PubMed: 15276680]

Voisey J, Van Daal A. Agouti: from man to mouse, from skin to fat. Pigment Cell Res 2002;15:10–18. [PubMed: 11837451]

Wang Y, Hirose K, Liberman MC. Dynamics of noise-induced cellular injury and repair in the mouse cochlea. J Assoc Res Otolaryngol 2002;3:248–268. [PubMed: 12382101]

Wangemann P. K+ recycling and the endocochlear potential. Hear Res 2002;165:1–9. [PubMed: 12031509]

Wangemann, P.; Schacht, J. Homeostatic mechanisms in the cochlea. In: Dallos, P.; Popper, AN.; Fay, RD., editors. The cochlea. Springer-Verlag; New York: 1996. p. 130-185.

Ward WD, Duvall AJ. Behavioral and ultrastructural correlates of acoustic trauma. Ann Otol 1971;80:881–896.

Ward, WD.; Turner, CW. The total energy concept as a unifying approach to the prediction of noise trauma and its application to exposure criteria. In: Hamernik, RP.; Henderson, D.; Salvi, R., editors. New perspectives on noise-induced hearing loss. Raven Press; New York: 1982. p. 423-435.

Wolters FLC, Klis SFL, de Groot JCMJ, Hamers FPT, Prieskorn DM, Miller JM, Smoorenburg GF. Systemic co-treatment with α-melanocyte stimulating hormone delays hearing loss caused by local cisplatin administration in guinea pigs. Hear Res 2003;179:53–61. [PubMed: 12742238]

Yamane H, Nakai Y, Takayama M, Iguchi H, Nakagawa T, Kojima K. Appearance of free radicals in the guinea pig inner ear after noise-induced acoustic trauma. Euro Arch Otorhinolaryngol 1995;252:504–508.

Yamasoba T, Goto Y, Komaki H, Mimaki M, Sudo K, Suzuki M. Cochlear damage due to germanium-induced mitochondrial dysfunction in guinea pigs. Neurosci Lett 2006;395:18–22. [PubMed: 16289317]

Yamasoba T, Kondo K, Miyajima C, Suzuki M. Changes in cell proliferation in rat and guinea pig cochlea after aminoglycoside-induced damage. Neurosci Lett 2003;347:171–174. [PubMed: 12875913]

Yoshida N, Hequembourg SJ, Atencio CA, Rosowski JJ, Liberman MC. Acoustic injury in mice: 129/SvEv is exceptionally resistant to noise-induced hearing loss. Hear Res 2000;141:97–106. [PubMed: 10713498]

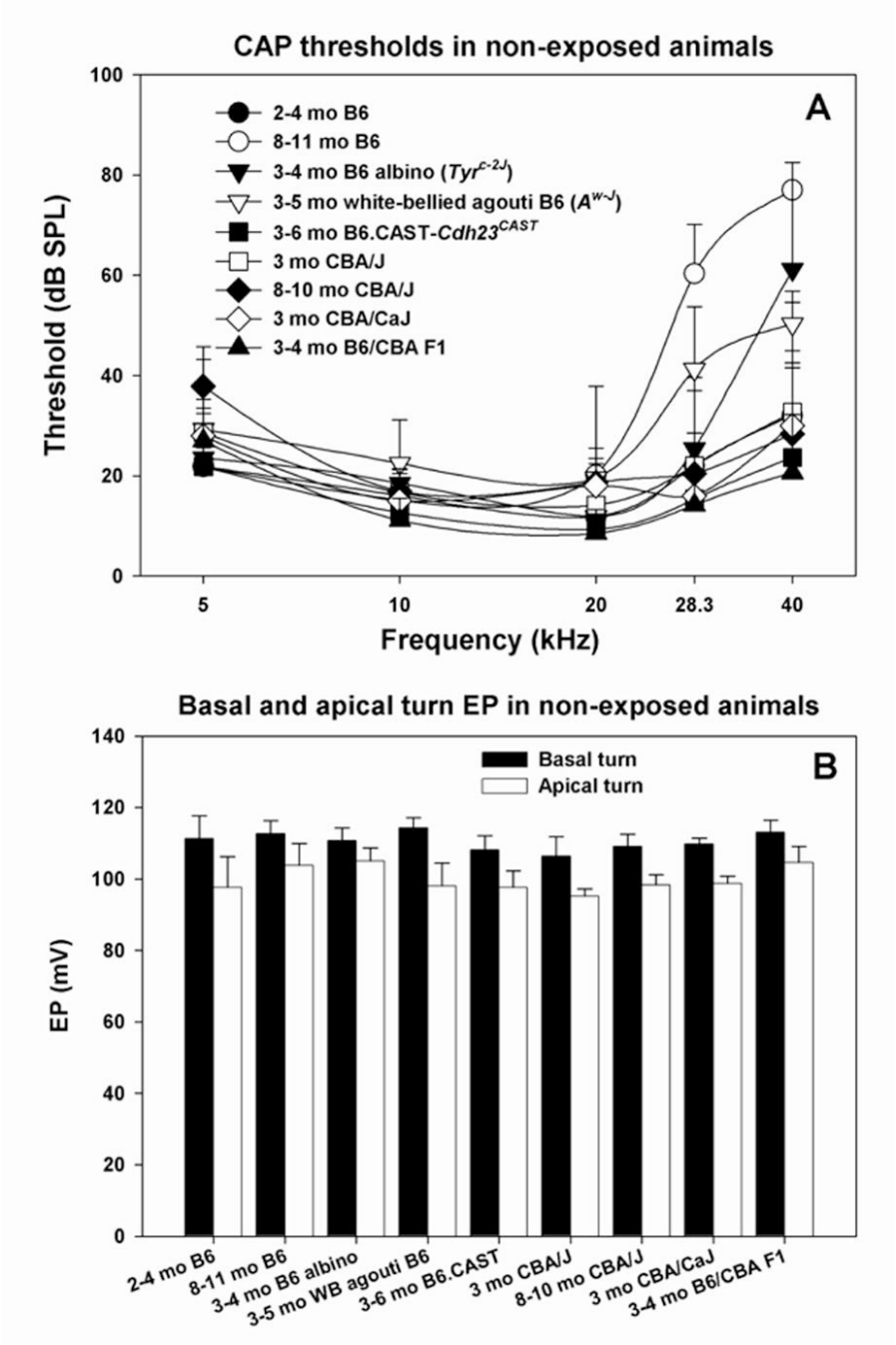

Figure 1.
A. Mean(+SD) CAP thresholds for unexposed controls of all mouse lines examined in the study. **B.** Mean (+SD) basal and apical turn EP values for the mice depicted in A.

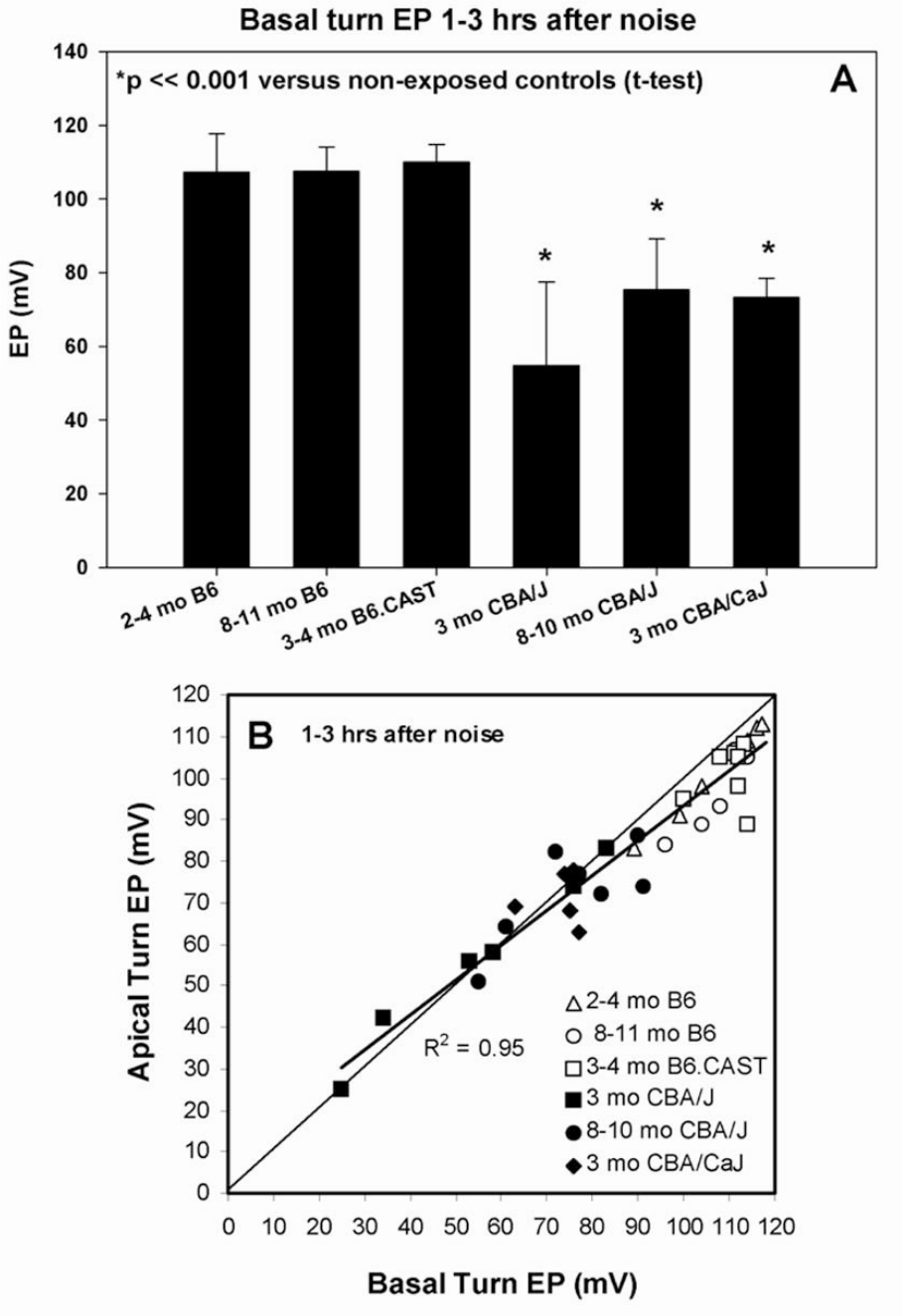

Figure 2.

A. Mean (+SD) basal turn endocochlear potentials measured 1–3 hrs after noise exposure in young and old B6, B6.CAST-*Cdh23*^{CAST} congenics, young and old CBA/J, and young CBA/CaJ mice. Only CBA mice showed significant EP reduction versus non-exposed controls of the same strain. **B.** Basal turn EP versus apical turn EP for the mice depicted in A. The normal spatial gradient for EP is preserved in B6 mice, but eliminated or reversed in CBAs, which show almost complete separation from B6.

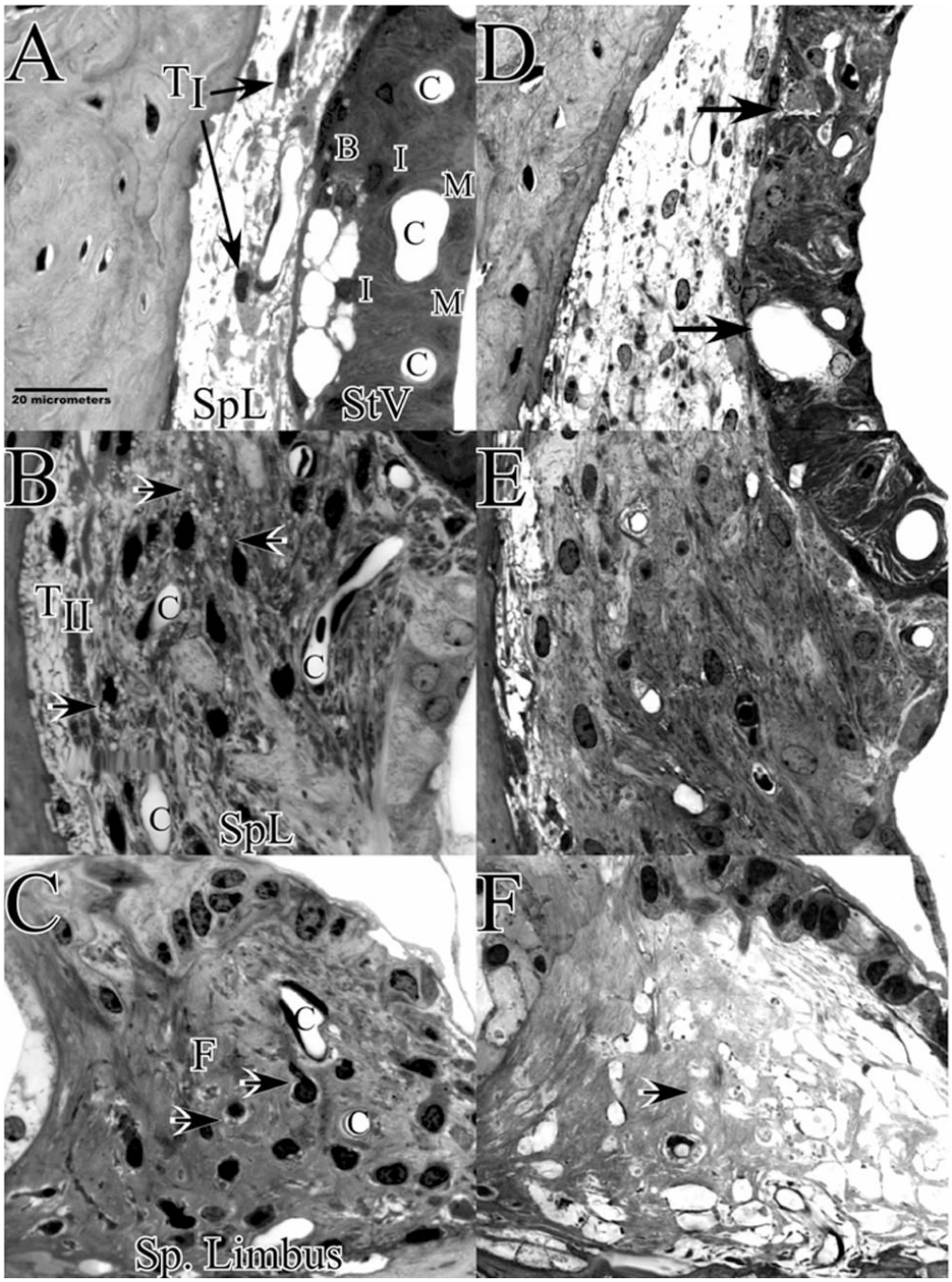

Figure 3.

Cochlear upper basal turn lateral wall and spiral limbus in example CBA/J mice 1–3 hrs after noise (A–C), or 8 wks after noise (D–F). **A.** Acutely, CBAs show shrinkage of Type I fibrocytes (arrows) and vacuolized basal cells within stria vascularis. **B.** Type II fibrocytes in spiral ligament contain vacuoles (arrows). **C.** Spiral limbus shows shrinkage of fibrocytes in the central zone (arrows). This was seen in both CBA and B6 and was present to some extent in control mice. **D.** At 8 wks the most obvious feature of the lateral wall is appearance of voids and extracellular debris within the stria (arrows). Stria is also notably thinner. **E.** Type II region of spiral ligament appears generally normal. **F.** Spiral limbus is completely devoid of

fibrocytes. T_I and T_{II}: Type I and II fibrocytes; SpL: Spiral ligament; StV: Stria vascularis; B: Basal cell layer; I: Intermediate cell layer; M: Marginal cell layer; C: Capillary.

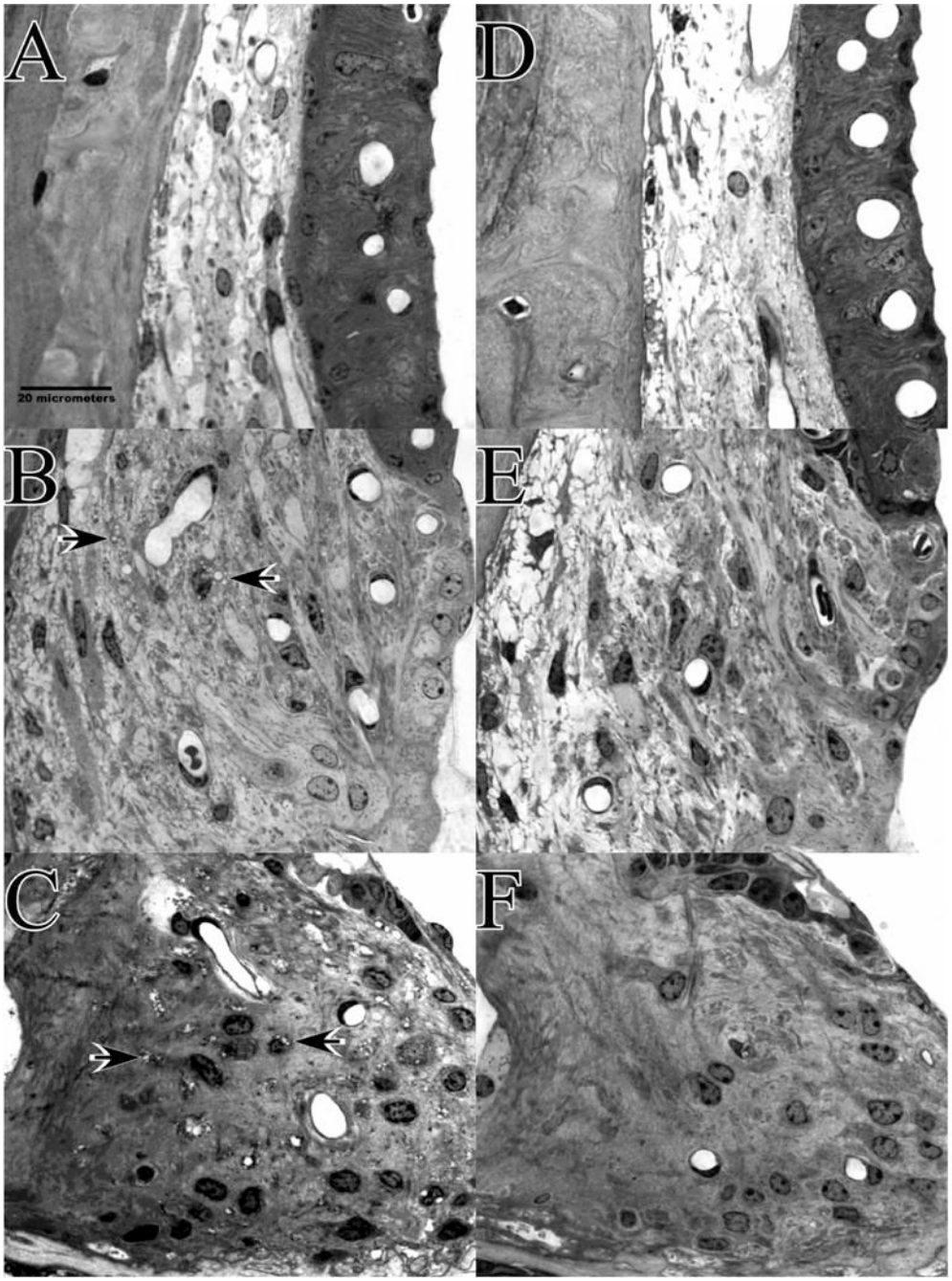

Figure 4.

Appearance of cochlear upper basal turn lateral wall and spiral limbus in example B6.CAST mice 1–3 hrs after noise (A–C), or 8 wks after noise (D–F). **A.** Acutely, stria vascularis and adjacent spiral ligament appear normal. **B.** Some Type II fibrocytes in spiral ligament contain vacuoles (arrows) but to a much more limited extent than in CBAs. **C.** Spiral limbus shows vacuolization of fibrocytes in the central zone (arrows). Like the shrinkage shown in Figure 3C, this was seen in both CBA and B6 and was present to some extent in control mice. **D.** At 8 wks stria and adjacent ligament appear normal. **E.** Type II region of spiral ligament appears generally normal. **F.** Spiral limbus shows no significant loss of fibrocytes.

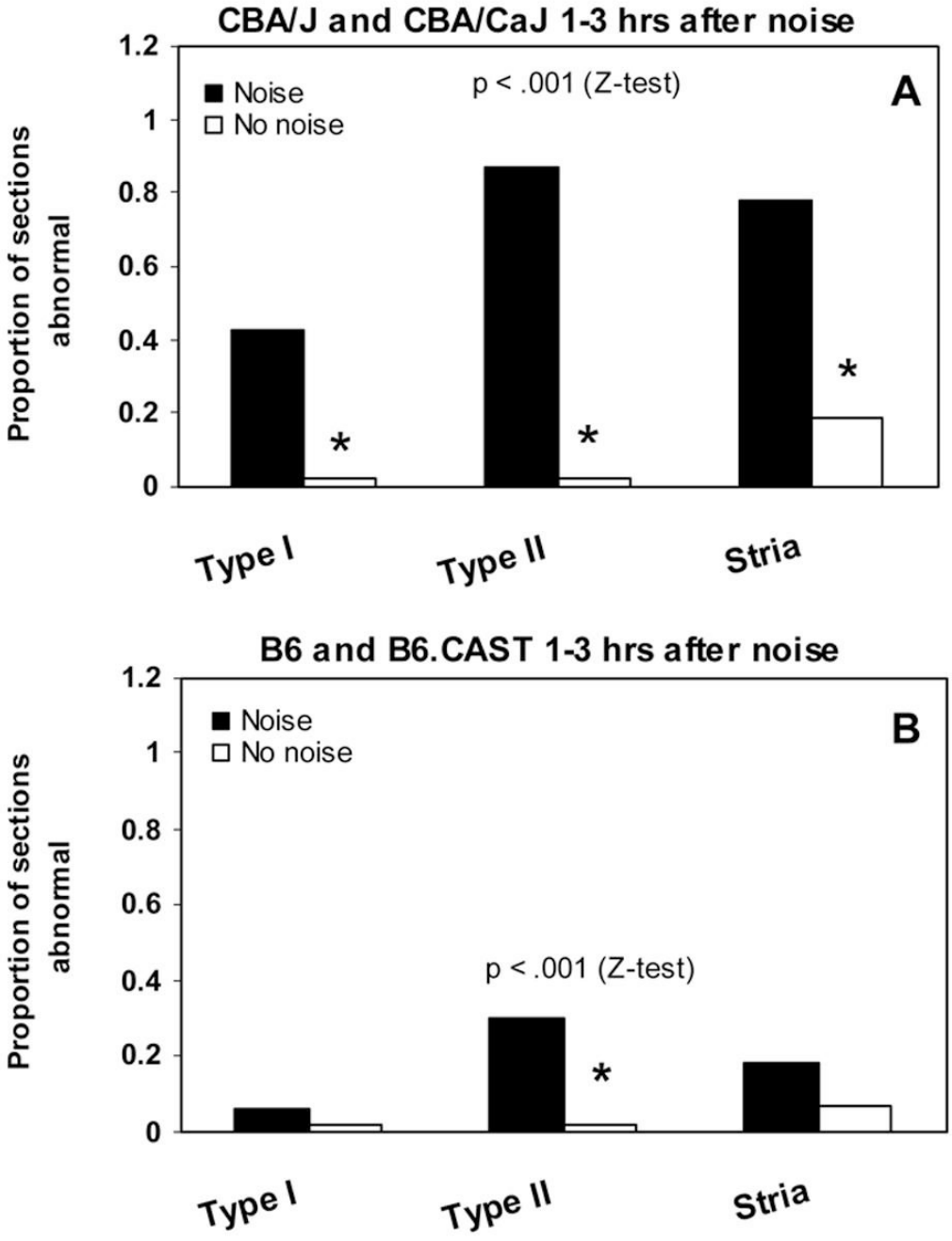

Figure 5.

Incidence of abnormalities of spiral ligament and stria vascularis in CBA (A) and B6 mice (B) 1–3 hrs after noise exposure. Sections were blindly scored based on appearance of Type I fibrocytes (shrinkage) and Type II fibrocytes (vacuoles) in ligament and presence of vacuoles in the stria. **A.** Noise-exposed CBA mice showed significant increase in the presence of all three types of anomalies versus non-exposed controls. **B.** Compared to non-exposed controls, exposed B6 mice showed significant increase only in the appearance of vacuoles in Type II fibrocytes, although at about 1/3 the incidence seen in CBAs.

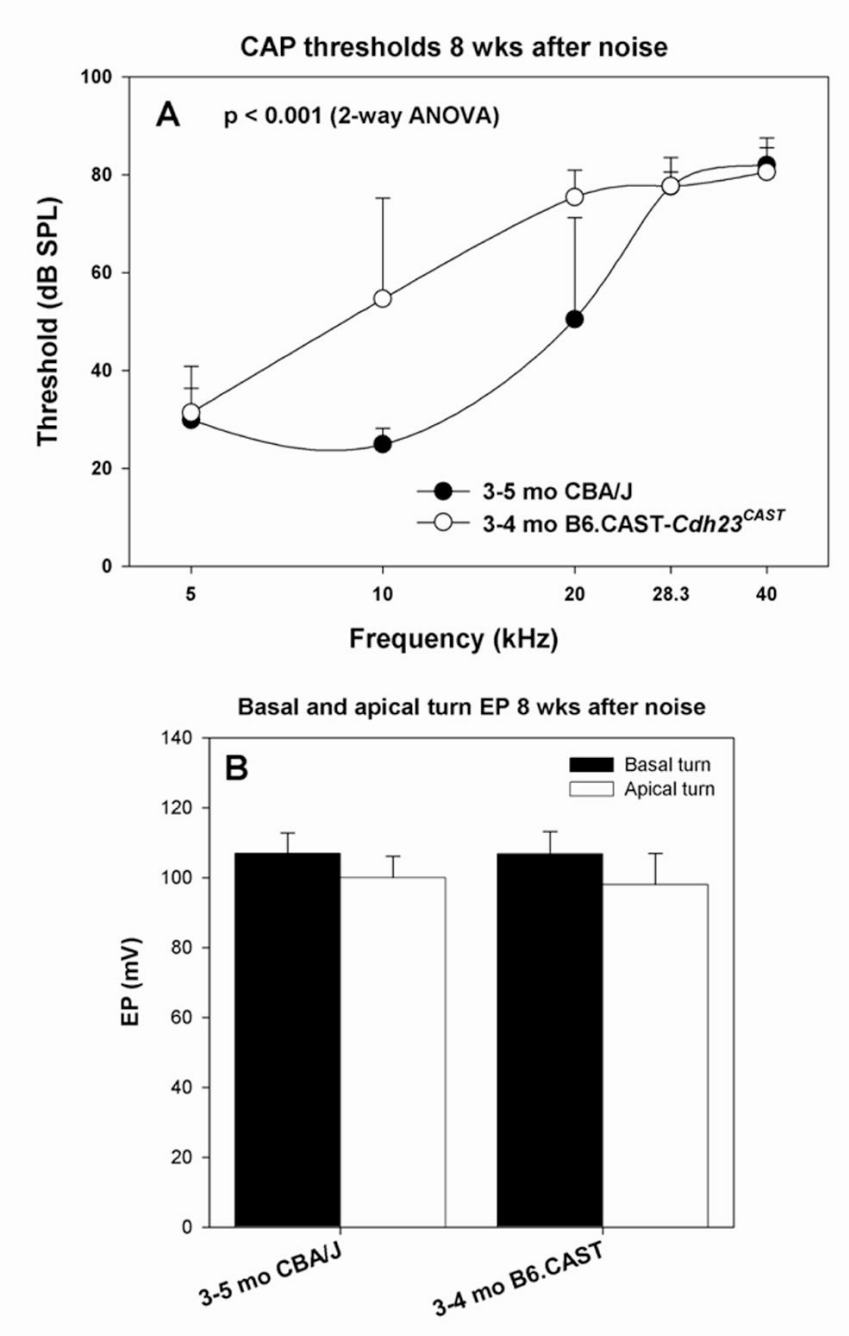

Figure 6.

Permanent physiological changes in CBA/J and B6.CAST mice with respect to CAP threshold (A) and basal and apical turn EP (B) measured 8 wks after noise exposure. **A.** B6.CAST mice showed significantly greater permanent threshold shifts than CBA/J (2-way ANOVA). **B.** Both strains showed EPs indistinguishable from non-exposed controls (t-test, $p>0.05$), indicating complete recovery.

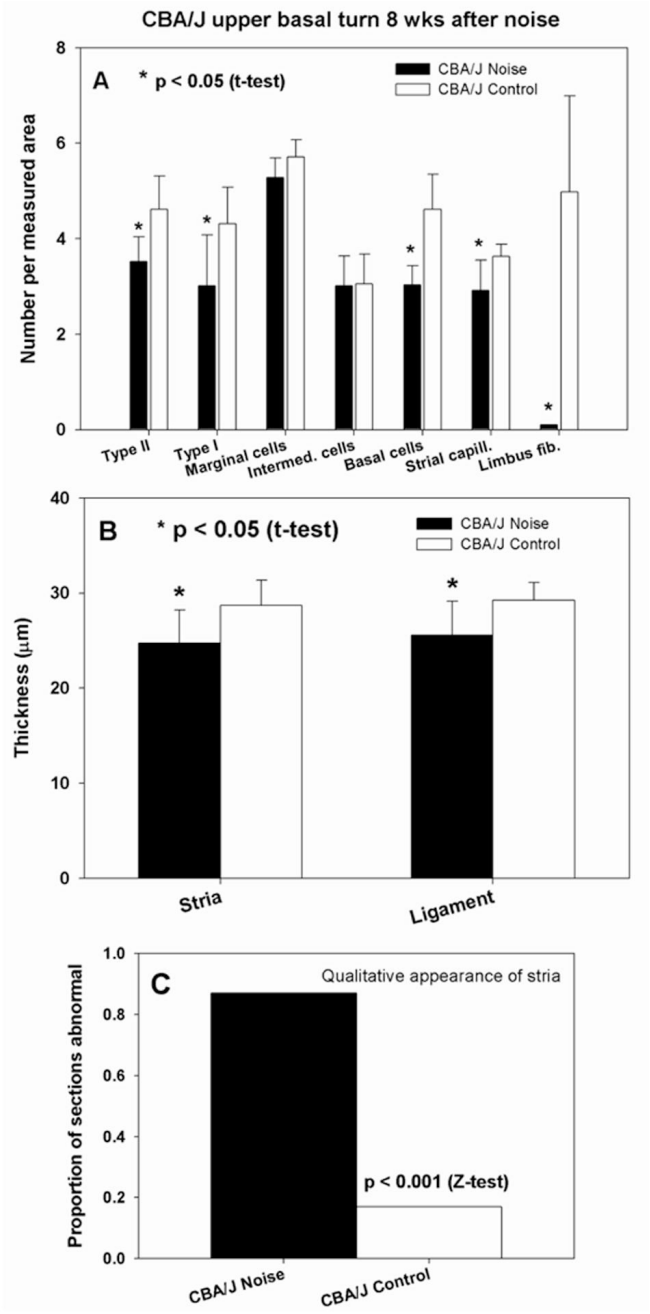

Figure 7.

Quantitative analysis of stria vascularis, spiral ligament, and spiral limbus in cochlear upper basal turn of CBA/J mice 8 wks after noise exposure. **A.** Versus non-exposed controls, noise exposed mice showed significant loss of Type I and II fibrocytes, strial basal cells, strial capillaries, and (nearly complete) loss of limbus fibrocytes. **B.** Stria and ligament were significantly thinner than in non-exposed controls. **C.** The incidence of strial abnormalities was significantly greater in noise exposed mice, increasing more than 4-fold.

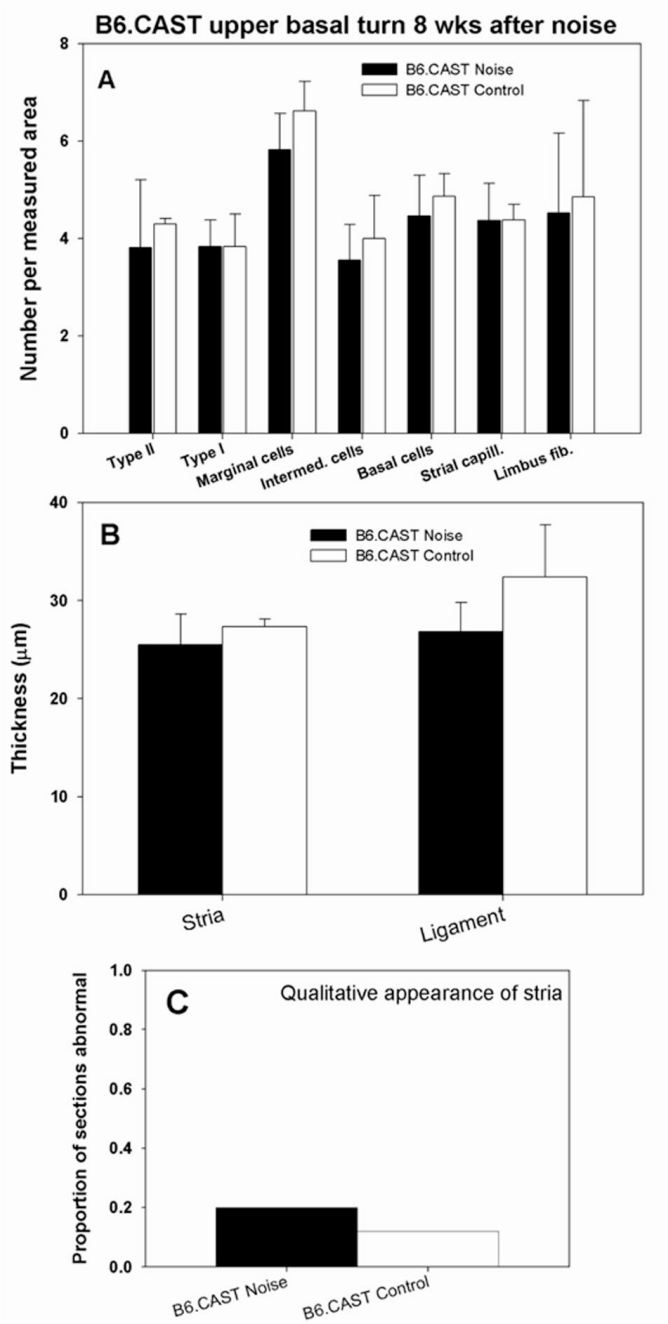

Figure 8.

Quantitative analysis of stria vascularis, spiral ligament, and spiral limbus in cochlear upper base of B6.CAST mice 8 wks after noise exposure. No anomalies were significant versus non-exposed controls (Compare with Figure 7.) Significant thinning of spiral ligament cannot be ruled out due to scatter of data (B).

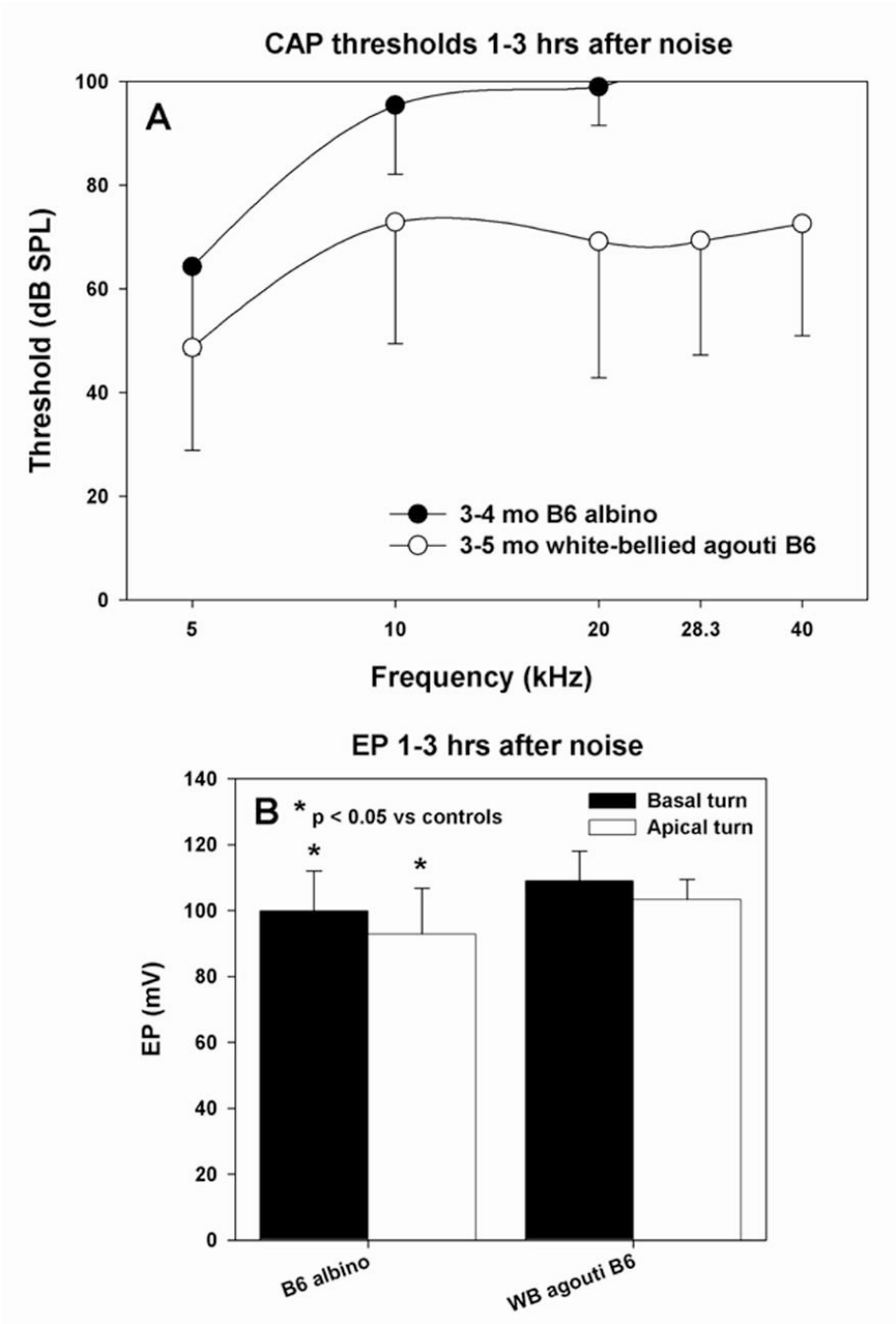

Figure 9.

Acute physiological changes in co-isogenic mice to B6 carrying alleles for albinism (C57BL/6-*Tyr*$^{c\text{-}2J}$) and white-bellied agouti (C57BL/6-*A*$^{w\text{-}J}$) with respect to CAP threshold (A) and basal and apical turn EP (B). **A.** Albinos showed acute threshold shifts similar to B6 parent strain, while agouti mice were resistant to threshold shifts. **B.** Versus non-exposed controls, noise-exposed albinos showed modest but significant reduction in EP in both cochlear turns. Agouti mice showed a statistically normal EP.

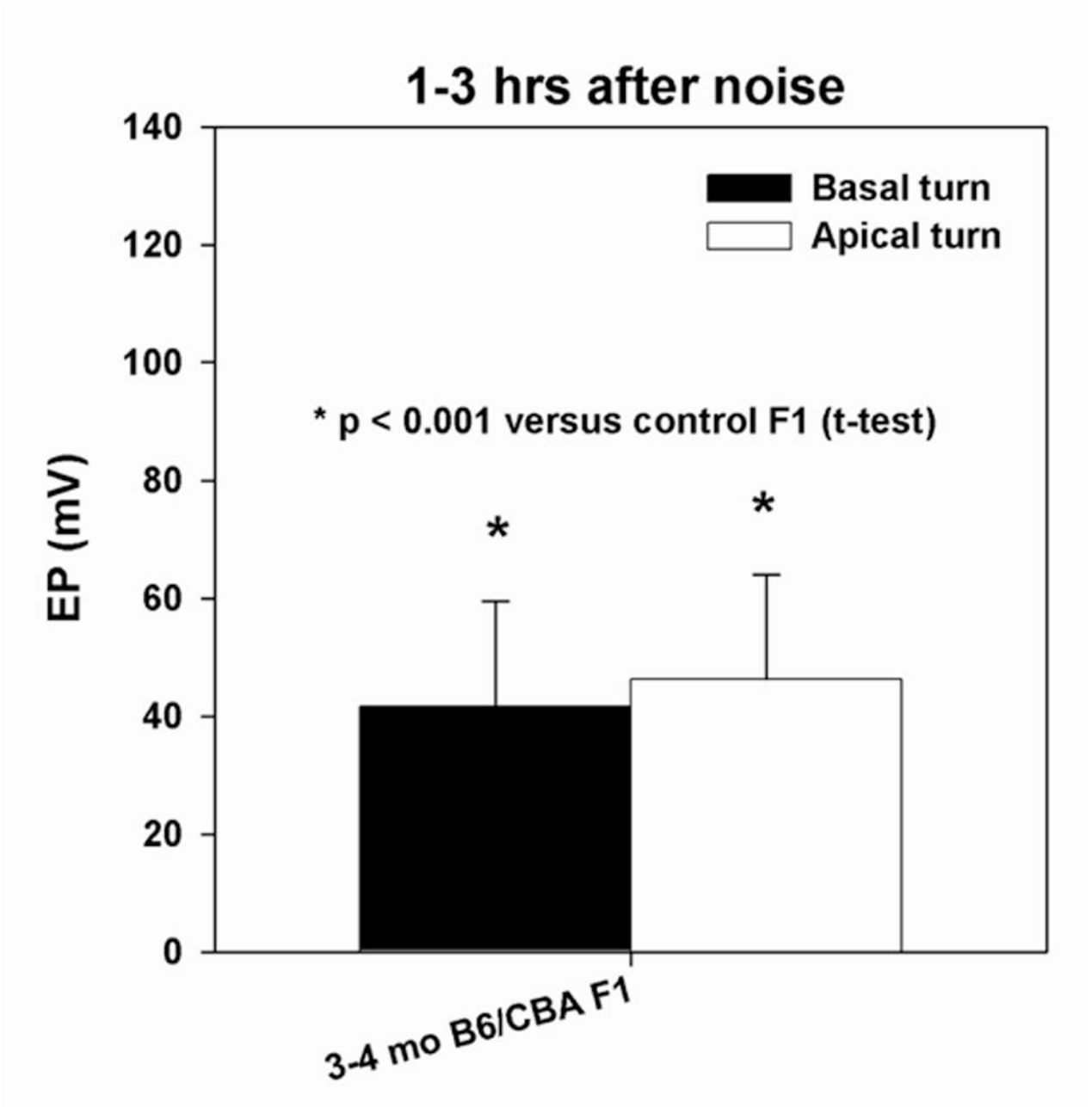

Figure 10.
Basal and apical turn endocochlear potential in B6xCBA F1 mice measured 1–3 hrs after noise exposure. The EP in both turns was significantly reduced compared to unexposed F1s.

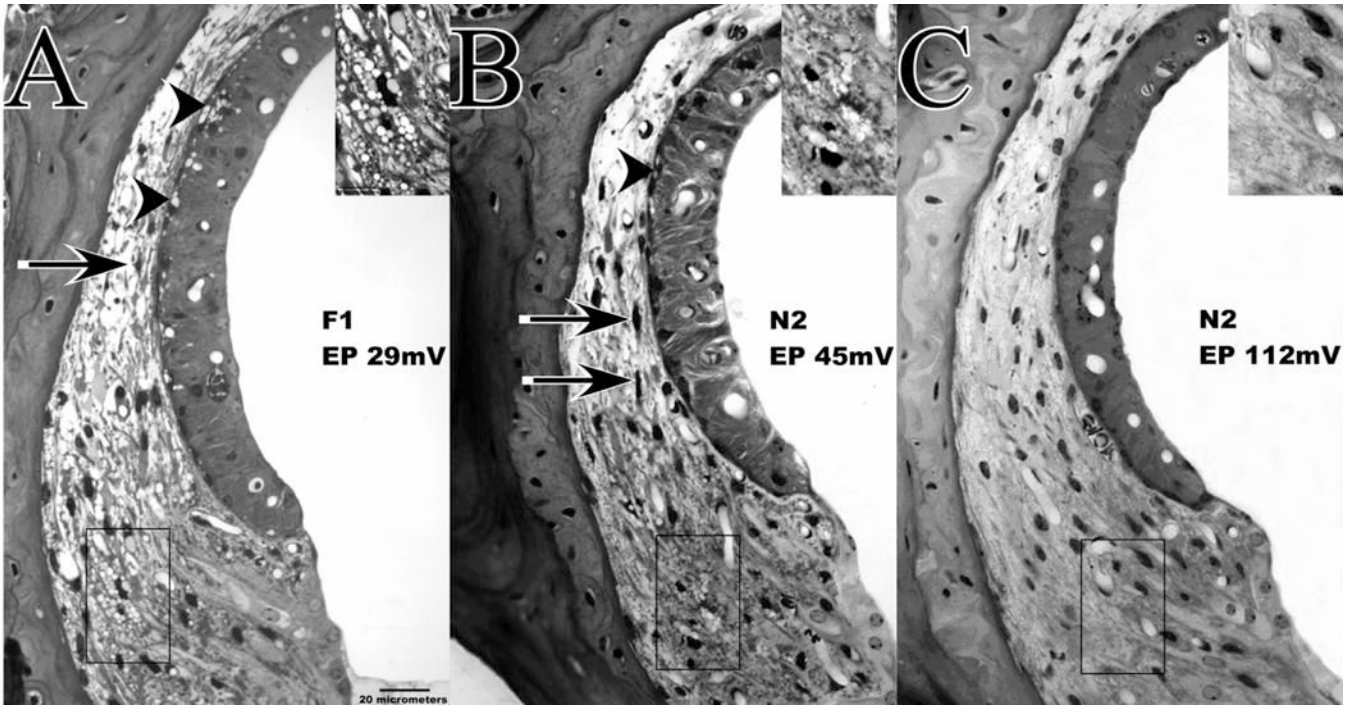

Figure 11.
Lateral wall of cochlear upper basal turn and EPs in F1 (A) and N2 (B,C) mice examined 1–3 hrs after noise exposure. Insets show expanded view of indicated Type II fibrocyte region of spiral ligament. N2 mice were chosen to illustrate the range of EP values and acute injury seen in these. Both the F1 featured in A and the N2 having a depressed EP (B) show CBA-characteristic acute pathology of spiral ligament and stria vascularis, including vacuolized Type II fibrocytes, shrunken Type I fibrocytes (arrows), and vacuolized strial basal cells (arrowheads). The N2 showing a normal EP (C) shows none of these features.

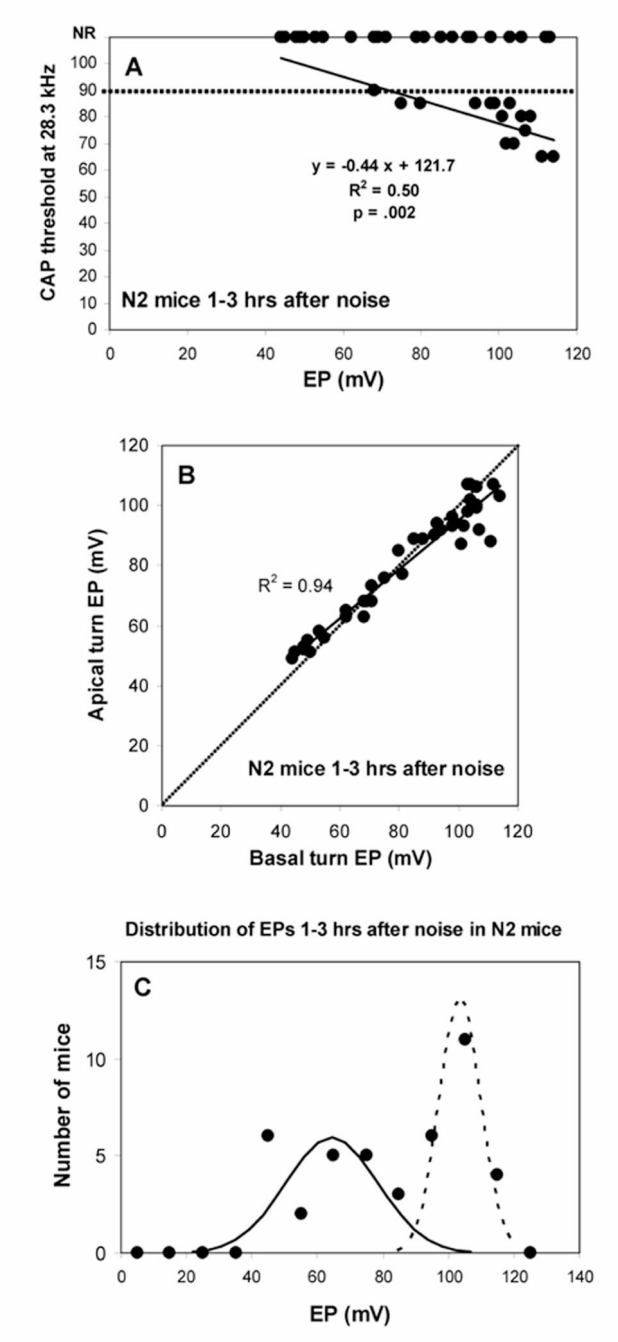

Figure 12.

Physiological measures in N2 backcross mice measured 1–3 hrs after noise exposure. **A.** CAP threshold at 28.3 kHz versus basal turn EP. Roughly half the animals showed no CAP response, largely independent of EP. Among mice showing a response, there was a significant negative correlation between threshold and EP, indicating an impact of the EP on acute threshold shifts. The dotted line indicates that maximum output of the sound system at 28.3 kHz. **B.** Basal turn EP versus apical turn EP for the animals depicted in A. As also shown in Figure 2, the normal spatial gradient for the EP is altered when the EP is reduced by noise exposure. **C.** Distribution of basal turn EP values for the same animals. EPs were sorted into 10 mV bins. 21 of 42 mice showed EPs below 90 mV; 21 showed higher EPs. Distribution was not normal, but was well

fit by two Gaussians with mean±SD of 64.3±14.1 mV (‘depressed EP’ cluster) and 103.5±6.3 mV (‘normal EP’ cluster).

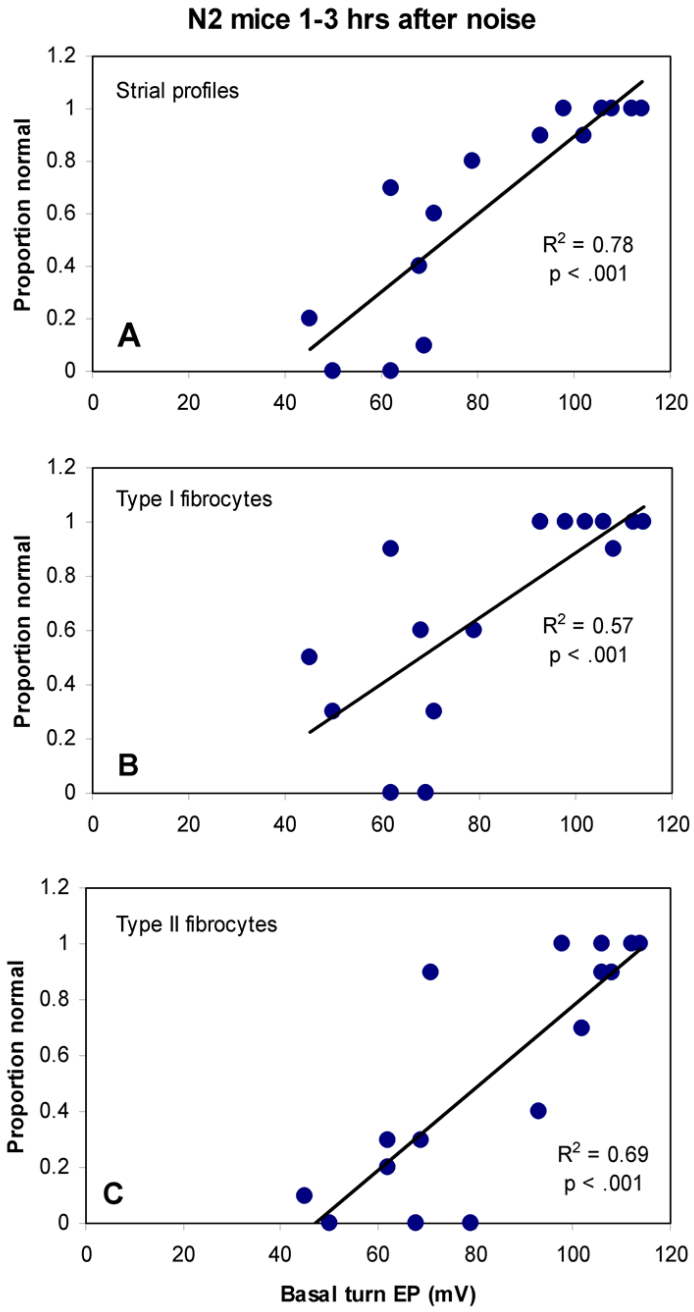

Figure 13.

Incidence of acute pathology of Type I and II fibrocytes and strial anomalies in N2 mice versus basal turn EP. Incidence of pathology (given as the proportion of sections that scored as normal) of stria vascularis (**A**), Type I (**B**), and Type II (**C**) was significantly correlated with EP by Pearson correlation.

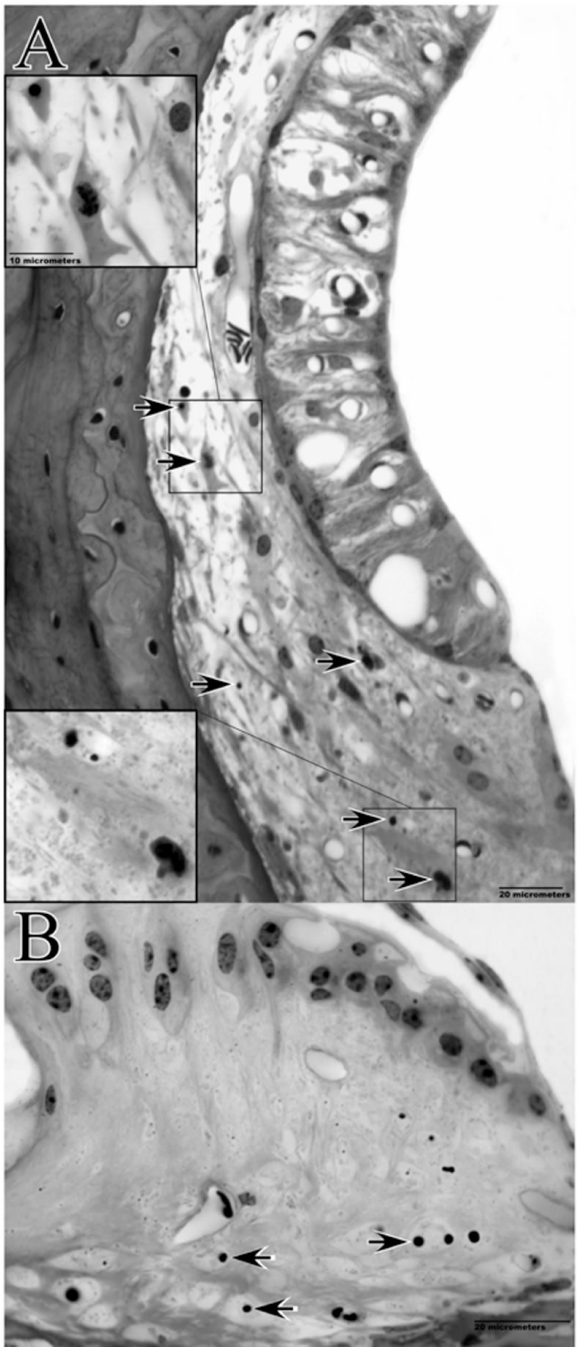

Figure 14.
Cochlear pathology observed 24 hrs post-noise exposure in example F1 hybrid mouse. The basal turn EP at the time of sacrifice was 50 mV. Lateral wall of the upper base (A) and spiral limbus of the lower apex (B) are shown. Note swollen intra-strial space, and pyknotic nuclei and dense cytoplasm of Type I and II fibrocytes (upper and lower insets, respectively, in A). B shows loss of cells and condensed nuclei of remaining cells in central zone of the limbus.

Table I

Sample size by strain, age, and experiment

Noise exposed mice received 2 hrs broadband (4–45 kHz) noise at 110 dB SPL. Groups were roughly equally mixed by gender.

Group	Initial age (mos)	Treatment			
		No-noise control	1–3 hrs after noise	24 hrs after noise	8 wks after noise
CBA/J	3	12 (6)	6 (6)		9 (6)
	8–10	12	7		
CBA/CaJ	3	5 (4)	6 (6)		
C57BL/6J	2–4	5 (4)	7 (5)		
	8–11	6	7		
B6.CAST-*Cdh23* ^{CAST}	3–6	12 (6)	7 (6)		14 (6)
C57BL/6J-*A* $^{w\text{-}J}$	3–5	4	7		
C57BL/6-*Tyr* $^{c\text{-}2J}$	3–4	6 (6)	12 (6)		
B6xCBA F1	3–4	8	11 (6)	8 (6)	
N2 backcross[#]	3–4	0	42 (17)		

[#][(B6.CASTxCBA) x B6.CAST] N2

Parentheses indicate number examined histologically.